Check for updates

Indium phosphide quantum dots as green nanosystems for environmental detoxification: surface engineering, photocatalytic mechanisms, and comparative material insights

Rima Heider Al Omari,[a] Anjan Kumar, [ID][b] Ali Fawzi Al-Hussainy,[c] Shaker Mohammed,[de] Aashna Sinha,[f] Subhashree Ray[g] and Hadi Noorizadeh [ID] *[h]

Indium phosphide (InP) quantum dots (QDs) offer a sustainable, low-toxicity alternative to heavy-metal-based nanomaterials for environmental detoxification. This critical review evaluates their potential as green photocatalysts, focusing on their ability to degrade organic pollutants, including dyes, pesticides, and polycyclic aromatic hydrocarbons (PAHs), under visible-light irradiation. Innovations in ligand functionalization, core/shell architectures, and eco-friendly synthesis enhance colloidal stability, photostability, and charge separation, surpassing traditional photocatalysts such as CdSe/ZnS and TiO_2 in efficiency and safety. By elucidating structure–property relationships, this work provides a novel framework for designing scalable, biocompatible nanomaterials, paving the way for advanced nanoremediation technologies to address global pollution challenges.

Environmental significance

This review highlights the transformative potential of indium phosphide (InP) quantum dots as eco-friendly photocatalysts for environmental detoxification, addressing the urgent need for sustainable solutions to combat organic pollutants such as dyes, PAHs, and pesticides. By synthesizing advancements in surface engineering, synthesis methods, and photocatalytic mechanisms, it underscores InP QDs' advantages over toxic cadmium-based alternatives, including low toxicity, visible-light activity, and robust aqueous stability. The critical evaluation of their performance, environmental fate, and safety offers a roadmap for designing scalable, green nanotechnology platforms. These insights are pivotal for developing efficient, regulatory-compliant remediation technologies, contributing to cleaner water systems and reduced ecological risks in complex environmental matrices. This is the first comprehensive review specifically addressing InP QDs in environmental detoxification.

1. Introduction

Environmental pollution resulting from industrial effluents, agricultural run-off, and urbanization has intensified the global need for efficient and sustainable remediation technologies.[1–5] Organic dyes, polycyclic aromatic hydrocarbons (PAHs), heavy metals, and pesticide residues pose significant risks to ecological systems and human health due to their persistence, toxicity, and bioaccumulation potential.[3–12] While conventional treatment strategies—such as activated carbon adsorption, membrane filtration, and chemical oxidation—have been widely employed, they often suffer from high energy consumption, low selectivity, secondary waste generation, and limited efficiency against emerging pollutants.[13–21]

Consequently, nanotechnology-based approaches have gained increasing attention as promising alternatives for next-generation environmental detoxification.[22–25] Among various nanomaterials, semiconductor quantum dots (QDs) have emerged as highly effective photocatalysts due to their size-tunable bandgaps, strong light absorption, high surface area, and photostability.[26–35] Traditionally, QDs composed of cadmium-based materials such as CdSe and CdTe have dominated the field, demonstrating exceptional photocatalytic and optoelectronic performance. However, the inherent toxicity and regulatory limitations associated with cadmium have led to

[a]Faculty of Allied Medical Sciences, Hourani Center for Applied Scientific Research, Al-Ahliyya Amman University, Amman, Jordan

[b]Department of Electronics and Communication Engineering, GLA University, Mathura-281406, India

[c]College of Pharmacy, Ahl Al Bayt University, Kerbala, Iraq

[d]College of Pharmacy, The Islamic University, Najaf, Iraq

[e]Department of Medical Analysis, Medical Laboratory Technique College, The Islamic University of Al Diwaniyah, Al Diwaniyah, Iraq

[f]School of Applied and Life Sciences, Division of Research and Innovation, Uttaranchal University, Dehradun, Uttarakhand, India

[g]Department of Biochemistry, IMS and SUM Hospital, Siksha 'O' Anusandhan (Deemed to Be University), Bhubaneswar, Odisha-751003, India

[h]Young Researchers and Elite Club, Tehran Branch, Islamic Azad University, Tehran, Iran. E-mail: hadinoorizadeh@yahoo.com

© 2025 The Author(s). Published by the Royal Society of Chemistry

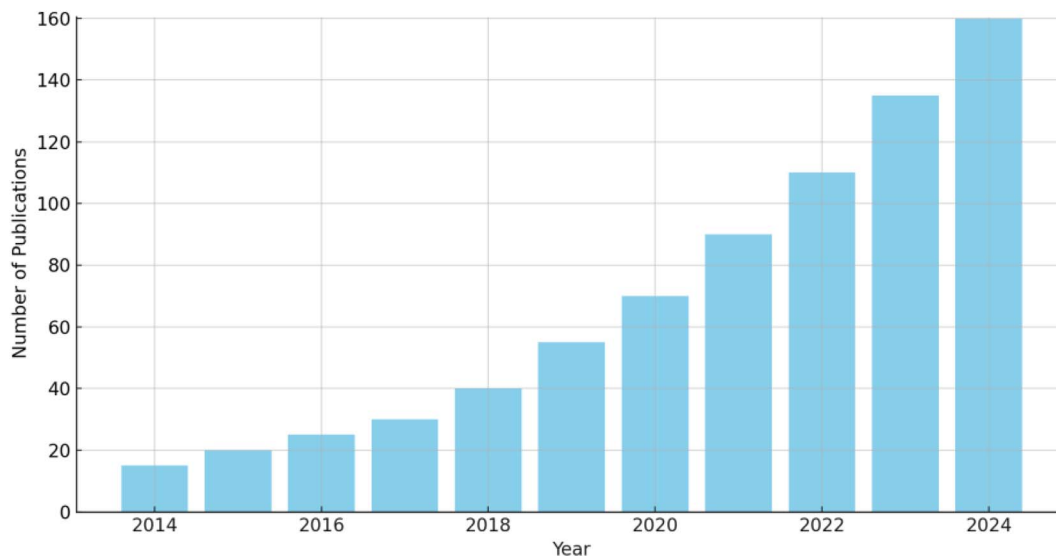*Environ. Sci.: Adv.*, 2025, 4, 1553–1586 | 1553

Fig. 1 Annual publications (2014–2024) on QDs in environmental applications.

growing concerns regarding their environmental and biomedical applications.[36–42]

This shift in regulatory and societal priorities has driven a surge of interest in developing heavy-metal-free alternatives that retain the functional advantages of QDs while minimizing ecological risks.[43–47]

To highlight the increasing research interest in this area, Fig. 1 presents the annual publication trends from 2014 to 2024 related to QDs in environmental applications. To underscore the growing research interest in this field, Fig. 1 illustrates the annual publication trends and citation counts for QDs in environmental applications from 2014 to 2024, drawing on data from papers.[48–62] These references highlight advancements in nanomaterial photocatalysis, including 2D materials, MXenes, *S*-scheme heterojunctions, and others, which provide a broader context for QD development. To enhance readability and provide

historical context, Table 1 presents a timeline of key academic research developments in InP QD synthesis, surface engineering, and environmental applications over the past decade. This timeline discusses general trends in nanomaterial synthesis and photocatalysis and highlights progress in green synthesis, core/shell engineering, and photocatalytic applications, offering a clear visual summary of QD research evolution.[57–64]

Addressing InP QD challenges requires a deep understanding of their surface chemistry, structural dynamics, and interfacial behavior. Advances in core/shell engineering, such as ZnS, ZnSe, and ZnSeS alloyed shells, have improved colloidal stability, oxidation resistance, and charge carrier lifetimes. Hydrophilic and zwitterionic ligands have enhanced aqueous dispersion across a wide pH and ionic strength range, enabling applications in wastewater and surface water systems. Multishell and graded-alloy structures, such as InP/ZnSe/ZnS or InP/$Zn_{0.25}Cd_{0.75}$S, have further boosted performance in environmental settings.[65,66] Synthesis techniques, including hot-injection, heat-up, microwave-assisted, and microfluidic methods, allow precise control over particle size, crystallinity, and surface ligand binding. Green and continuous-flow synthesis protocols align with sustainability goals by reducing hazardous reagents, energy use, and waste, promoting scalability for practical remediation.[67,68] The photocatalytic activity of InP QDs hinges on charge carrier dynamics—generation, separation, and transport of photoinduced electrons and holes. Band structure tailoring through alloying or doping, surface state engineering, and integration with conductive matrices (*e.g.*, TiO_2, g-C_3N_4, or MXenes) enhance reactive oxygen species (ROS) formation, pollutant adsorption, and degradation rates. InP-based systems have shown impressive performance in degrading organic dyes, PAHs, and pesticides under visible-light irradiation, even under saline or complex wastewater conditions.[69,70] Fig. 2 illustrates InP QDs for photocatalytic pollutant degradation, highlighting challenges and engineering strategies.

Dr. Hadi Noorizadeh is an Associate Professor of Analytical Chemistry. His research focuses on electrochemical sensors, quantum dots, nanochemistry, and quantitative structure–retention/activity relationships (QSRR/QSAR). With over 70 peer-reviewed publications, he advances environmental and pharmaceutical analysis. Dr Noorizadeh is a regular reviewer for international journals, an invited speaker at global conferences, and has supervised numerous M.Sc. and Ph.D. students. He holds expertise in chemometrics and electrochemical techniques (CV, DPV, and EIS), contributing to innovative sensor designs for pollutant detection.

Hadi Noorizadeh

Table 1 Timeline of academic research developments in InP QDs for environmental applications

Year	Milestone	Description
2014	Early exploration of InP QDs	Initial studies on InP QD synthesis and optoelectronic properties, establishing them as cadmium-free alternatives, inspired by advances in 2D material synthesis techniques (*e.g.*, CVD growth)
2016	Advances in surface passivation	Development of ZnS and ZnSe shells to enhance photostability and reduce surface defects, improving aqueous compatibility, paralleling surface modification strategies for non-oxide photocatalysts
2018	Green synthesis methods	Adoption of safer precursors (*e.g.*, tris(dimethylamino)phosphine) and ligand-assisted approaches for eco-friendly InP QD production, aligning with sustainable nanomaterial synthesis trends
2020	Core/shell engineering	Optimization of multi-shell (*e.g.*, InP/ZnSe/ZnS) and graded-alloy structures to improve charge separation and photocatalytic efficiency, drawing on heterostructure design principles from MXenes
2022	Photocatalytic applications	Demonstration of InP QDs for efficient degradation of organic dyes and PAHs under visible-light irradiation in complex aqueous environments, leveraging insights from *S*-scheme heterojunction photocatalysis
2023	Scalable synthesis techniques	Adoption of microfluidic and continuous-flow synthesis for reproducible, high-throughput InP QD production, reflecting scalable fabrication strategies for 3D porous carbon-based materials and MXenes
2024	Environmental stability and toxicity	Studies on InP QD stability under high-salinity and variable pH conditions, with reduced ecotoxicity through advanced surface engineering, informed by environmental safety assessments of MXene/CNT hybrids and electro-Fenton processes

Despite advances in photocatalytic nanomaterials, significant gaps remain in the literature regarding InP QDs for environmental detoxification. Existing studies on cadmium-based QDs and traditional photocatalysts such as TiO₂ lack a unified approach to address eco-friendly synthesis, surface engineering,

Fig. 2 InP QDs synthesized *via* green methods, surface-engineered for visible-light-driven degradation of pollutants, with lower toxicity and higher efficiency than conventional photocatalysts.

and scalable applications. Reviews on related materials, such as nitrogen-doped magnetic biochar and graphdiyne, highlight the need for integrated strategies to enhance efficiency and sustainability. This review fills this gap by being the first comprehensive synthesis of InP QD research, benchmarking their performance against CdSe/ZnS and TiO₂, and proposing a predictive model for optimization. These contributions provide a novel framework for designing safe, scalable nanotechnology solutions, addressing current limitations in water remediation research. We explore how structural and interfacial modifications impact photocatalytic behavior, assess the environmental fate and stability of these nanostructures, and benchmark their performance against conventional and emerging nanomaterials. By integrating insights from materials chemistry, environmental science, and surface/interface engineering, this work aims to guide the rational design of InP QDs for sustainable remediation technologies. The implications extend beyond laboratory-scale demonstrations, offering pathways toward safe, scalable, and high-efficiency nanotechnologies for addressing global pollution challenges.
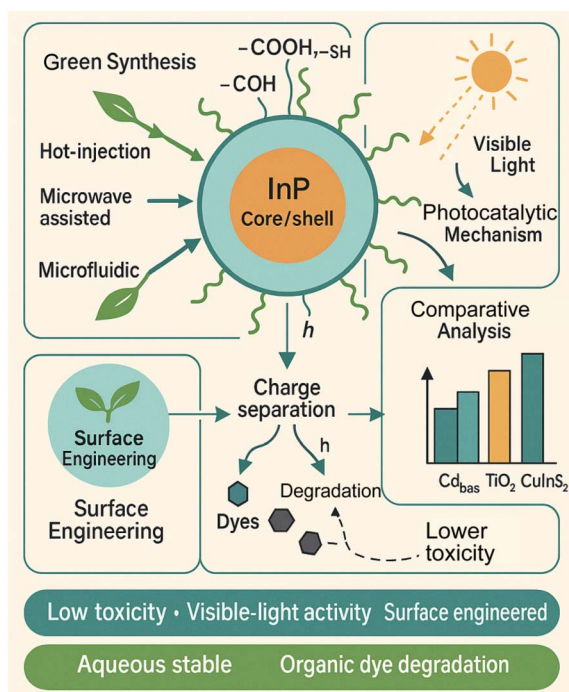
2. Structural and surface chemistry of InP quantum dots

2.1. Core crystal structure and quantum confinement behavior

InP QDs are direct-bandgap III–V semiconductor nanocrystals that typically adopt a zinc-blende structure, although wurtzite polymorphs have also been observed under specific synthetic regimes.[71–73] The crystalline phase of InP is governed by parameters such as precursor reactivity, ligand coordination, and reaction temperature, all of which influence the thermodynamic favorability of a given lattice configuration. In their

© 2025 The Author(s). Published by the Royal Society of Chemistry

Environ. Sci.: Adv., 2025, **4**, 1553–1586 | **1555**

quantum-confined regime (typically < 10 nm), InP QDs exhibit size-dependent optoelectronic properties due to the discretization of energy levels resulting from confinement of charge carriers in all three spatial dimensions.[74–76] Quantum confinement leads to a blue shift in both absorption onset and photoluminescence (PL) peak as particle diameter decreases. This behavior can be quantitatively described using the effective mass approximation (EMA), wherein the bandgap energy increases inversely with the square of the QD radius, although deviations occur at very small sizes due to surface states and non-parabolic band structures. The electron and hole effective masses in InP are notably asymmetric (0.077 and 0.6 m_e, respectively), influencing the excitonic Bohr radius ($\sim$10 nm) and thus the size range over which quantum effects dominate.[77,78] Additionally, alloying and strain effects induced by surface reconstruction or lattice mismatches further modulate the band edge energies, a phenomenon that becomes critical when designing QDs for photocatalysis or sensing applications.[79–82] Three prototypical band alignment configurations are observed in core/shell QD heterostructures: Type I, Type II, and Quasi-Type II. In Type I structures, both the electron and hole are confined within the core due to favorable band alignment, resulting in strong spatial overlap and efficient radiative recombination.[83,84] Type II configurations, by contrast, spatially separate the electron and hole across the core–shell interface, promoting charge separation and thereby extending exciton lifetimes—a feature advantageous for photocatalysis. The Quasi-Type II system represents an intermediate case, where typically only one carrier (usually the electron) delocalizes into the shell, modulating recombination dynamics and energy transfer efficiency.[85,86]

The relative band edge positions of common II–VI and III–V semiconductor materials (*e.g.*, ZnS, ZnSe, InP, CdS, and CdSe) can be considered on an absolute energy scale referenced to the vacuum level. This energy alignment is critical for rational heterostructure design, as it determines the nature of charge confinement and separation. Materials such as ZnS and ZnSe, with deeper valence band maxima and higher conduction band minima, often serve as effective shell materials for Type I structures due to their wider bandgaps. Meanwhile, staggered alignments with materials such as CdSe or InP enable the realization of Type II or Quasi-Type II architectures, where asymmetry in carrier localization is exploited for specific electronic and photophysical properties. Normalized PL spectra for core/shell QDs with increasing shell thickness (in monolayers, ML) of ZnS and ZnSe demonstrate key optical properties.[87–89] A pronounced red shift in the PL peak is observed with increasing shell thickness, indicative of modified quantum confinement and dielectric screening effects. For the ZnS system, the emission red-shift is accompanied by spectral narrowing, consistent with reduced nonradiative recombination due to surface passivation. Similarly, ZnSe shell growth leads to tunable emission, underlining the impact of shell composition and thickness on excitonic recombination dynamics. These optical tunabilities are pivotal when optimizing QDs for optoelectronic and energy-harvesting applications.[90,91]

From a crystallographic standpoint, high-resolution transmission electron microscopy (HRTEM) typically reveals well-defined lattice fringes consistent with a face-centered cubic (FCC) phase. However, during the rapid burst of nucleation, particularly in hot-injection methods, stacking faults and twin planes may develop, disrupting the periodic potential and serving as trap sites.[70,92] Such structural irregularities introduce shallow or deep defect states within the bandgap, decreasing PLQY and reducing carrier mobility—detrimental effects that compromise photocatalytic efficiency. The suppression of these defects demands meticulous control over precursor conversion kinetics, ligand–shell interactions, and thermal gradients within the reaction medium.[93–95] Furthermore, anisotropy in growth rates along different crystallographic axes can lead to non-spherical morphologies such as rods or tetrahedra, especially in ligand-rich environments where facet-selective passivation occurs. Such morphological deviations affect the spatial localization of electronic wavefunctions, the dipole moment distribution, and the surface-area-to-volume ratio—all of which critically determine reactivity and interaction with environmental species. These morphological and structural considerations form the foundational framework upon which surface and interface chemistry must be engineered.[96–98] Furthermore, the incorporation of alloyed $Zn_{0.25}Cd_{0.75}S$ shells has been demonstrated to confer exceptional colloidal stability and high photocatalytic performance of InP-based QDs under real wastewater treatment conditions. This structural adaptation effectively mitigates surface oxidation and ensures long-term functionality in harsh aquatic environments.[99,100]

2.2. Surface defects and native oxide formation

Despite advances in core crystallinity, surface defects remain the Achilles' heel of InP QDs, substantially limiting their photostability, catalytic efficiency, and biocompatibility. Unlike II–VI QDs, where ionic bonding dominates, InP surfaces exhibit a high density of covalent dangling bonds and under-coordinated sites. These defects arise from incomplete surface coverage, lattice truncation, and thermally activated desorption events during synthesis or purification. Unpassivated phosphorus and indium atoms on the surface readily react with ambient oxygen or water, forming indium oxide (In_2O_3), phosphates (PO_4^{3-}), or mixed-oxidation-state phosphates ($InPO_4$), which introduce deep electronic trap states.[101–103] X-ray photoelectron spectroscopy (XPS) studies consistently detect peaks associated with oxidized phosphorus species even in freshly prepared QDs, suggesting that oxidation occurs almost immediately after synthesis, particularly during purification or air exposure. These oxides induce mid-gap states that promote non-radiative Auger recombination, significantly quenching PL and shortening exciton lifetimes—effects that are particularly deleterious in photocatalytic or sensing environments. Moreover, these oxide layers hinder effective electronic communication between the QD and electron acceptors or cocatalysts, severely limiting charge transfer efficiency.[104–106]

Fig. 3a presents a representative transmission electron microscopy (TEM) image of the as-synthesized InP QDs, clearly
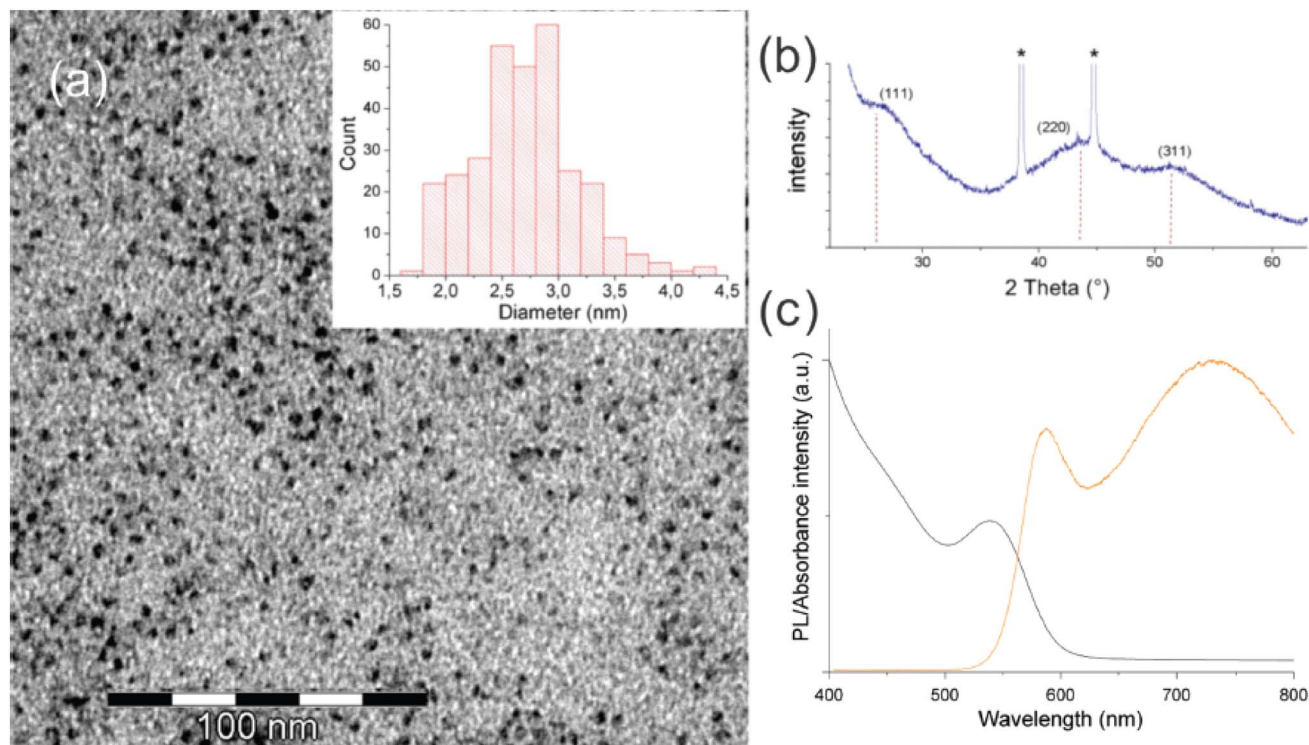
Fig. 3 (a) TEM image and size distribution of InP QDs (∼2.7 nm); (b) XRD pattern showing the zinc blende crystal structure; (c) UV–Vis absorption and PL spectra highlighting band–edge emission (∼590 nm) and surface trap emission (∼710 nm). Reproduced with permission from ref. 105, copyright 2023 American Chemical Society.

illustrating their spherical morphology and uniform dispersion. The associated size distribution histogram (inset) confirms a narrow diameter range centered around 2.7 ± 0.5 nm, which is critical for controlling surface-to-volume ratios that influence both surface reactivity and defect density.[105] This size uniformity is particularly relevant in the context of defect engineering, as smaller QDs inherently possess a greater proportion of surface atoms, thus increasing susceptibility to the formation of undercoordinated sites and native oxides. Given the high surface energy of InP and its sensitivity to oxidative conditions during post-synthetic purification, these structural observations underscore the importance of surface stabilization strategies to mitigate uncontrolled formation of In_2O_3 or $InPO_4$ phases. Fig. 3b displays the X-ray diffraction (XRD) pattern of the InP QDs, featuring broad reflections characteristic of nanocrystalline domains and indexing to the zinc blende crystal structure. The (111), (220), and (311) diffraction planes are evident, although peak broadening is pronounced due to the nanoscale size, which aligns with the Scherrer effect. Notably, these diffraction features confirm the presence of a well-formed crystalline core, but do not preclude the existence of an amorphous or partially oxidized surface layer. The absence of distinct signals from oxide phases suggests that native oxide formation, while pervasive at the surface (as corroborated by XPS and solid-state NMR in the full study), remains below the detection threshold of XRD. This disparity highlights the necessity of complementary surface-sensitive spectroscopies to detect ultrathin oxide layers or substoichiometric surface species that

adversely affect charge carrier dynamics. Fig. 3c illustrates the optical absorption and PL spectra of the InP QDs, revealing two key emissive features: a sharp excitonic peak near 590 nm and a broader, red-shifted band centered around 710 nm. The narrow excitonic emission corresponds to band-edge recombination within the crystalline core, whereas the lower-energy emission is attributed to radiative transitions involving surface trap states, often associated with undercoordinated indium atoms or oxidized phosphorus moieties. These mid-gap states act as recombination centers that quench PL efficiency, consistent with the proposed model of defect-mediated non-radiative Auger recombination. The co-existence of these emissions underscores the duality of the InP QDs' surface: a crystalline interior capable of efficient quantum confinement and a chemically reactive periphery susceptible to oxidation, which together dictate the photostability and catalytic viability of the nanocrystals in real-world applications.

Importantly, toxicological assessments of InP/ZnS core/shell structures have also confirmed their stability and reduced adverse effects in aqueous systems, supporting their environmental compatibility and functional deployment in detoxification applications. These findings further validate the robustness of surface-engineered InP-based QDs under diverse aquatic conditions.[106–108] Additionally, surface reconstruction phenomena can alter the local coordination environment. Density functional theory (DFT) calculations indicate that indium-rich facets tend to exhibit metallic surface states, whereas phosphorus-terminated surfaces favor insulating

© 2025 The Author(s). Published by the Royal Society of Chemistry

Environ. Sci.: Adv., 2025, **4**, 1553–1586 | **1557**

character. These reconstructions are dynamic and can change upon ligand desorption, pH fluctuations, or interaction with redox species in environmental matrices. Furthermore, the presence of acidic or basic species (*e.g.*, H^+, OH^-, or carbonate ions) can catalyze surface hydrolysis or promote the formation of metastable hydroxide intermediates, accelerating degradation under realistic environmental conditions.[109] Suppressing surface oxidation and defect formation has thus become a key target in InP QD engineering. Strategies include the use of tris(trimethylsilyl)phosphine [$(TMS)_3P$] or less pyrophoric alternatives such as tris(dimethylamino)phosphine (TDMP) under rigorously air-free conditions. Chelating ligands such as carboxylates, thiols, or phosphonates can passivate dangling bonds by forming stable coordination complexes with surface atoms. However, such ligands must simultaneously fulfill criteria of solubility, colloidal stability, and environmental compatibility—a trifecta rarely achieved without trade-offs.[110,111]

2.3. Strategies for surface passivation and shell engineering

To overcome the limitations imposed by native surface defects, post-synthetic surface passivation *via* epitaxial shell growth has emerged as a primary method for improving QD performance. Core/shell heterostructures such as InP/ZnS, InP/ZnSe, and InP/ZnSeS are designed to create favorable band alignments that confine excitons within the core, minimizing surface exposure and suppressing trap-mediated recombination.[112,113] The choice of shell material dictates not only the optical properties but also the mechanical stability and surface charge environment of the QDs.[114,115] However, epitaxial shelling is complicated by significant lattice mismatches between InP and typical shell materials. For instance, the ~7% mismatch between InP and ZnS can lead to interfacial strain, misfit dislocations, and partial amorphization—factors that generate non-radiative decay channels and compromise charge transport.[116–118] One approach to mitigate these effects involves gradient alloying, such as using $ZnSe_xS_{1-x}$ or ZnCdS shells, to gradually transition lattice parameters and reduce interfacial strain. These graded shells also facilitate smoother electronic band profiles, enabling efficient charge separation and energy transfer in catalytic applications.[119]

Advanced shell growth protocols such as successive ion layer adsorption and reaction (SILAR) or continuous injection methods have enabled precise control over shell thickness, composition, and uniformity. These protocols offer tunability over the energy offset at the core–shell interface, critical for aligning conduction or valence bands with redox potentials in photocatalysis.[120] In certain configurations, Type-II band alignment can be achieved, wherein electrons and holes are spatially separated into different regions of the QD, thereby extending carrier lifetimes and enhancing charge utilization.[110] Ligand engineering is an equally critical element of surface passivation. Native ligands such as oleic acid or trioctylphosphine are often replaced with short-chain or functionalized moieties (*e.g.*, dihydrolipoic acid, polyethylene glycol, or zwitterionic ligands) to improve solubility, facilitate interfacial interactions, or enable bioconjugation. In photocatalytic systems, electron-donating ligands can enhance carrier extraction, while hydrophilic moieties improve aqueous stability and dispersion.[121–123] Additionally, bifunctional ligands that serve both as passivators and anchoring agents for cocatalysts (*e.g.*, TiO_2 and carbon dots) enable the construction of hybrid nanocomposites with synergistic functionalities.[101] Notably, shell growth must be optimized to avoid electron/hole tunneling barriers that can restrict interfacial reactivity. Excessively thick shells, while improving stability, can insulate the core from the environment, rendering the QDs inactive in photocatalytic processes. Therefore, rational design must balance core protection with functional accessibility, especially under harsh chemical or photonic conditions encountered in real-world remediation scenarios.[124–128] Tailored ligand functionalization and core/shell designs significantly enhance InP QD stability and photocatalytic efficiency, offering a promising avenue for practical water remediation applications.

2.4. Comparative experimental characterization of InP QDs

InP QDs are pivotal in advancing non-toxic semiconductor technologies, with their optoelectronic properties tailored for applications in photonics, biosensing, and environmental catalysis. The performance of InP QDs hinges on a nuanced interplay of size, composition, and surface engineering, which is rigorously probed through advanced experimental characterization techniques.[129–133] TEM, with its nanoscale resolution, elucidates QD morphology and crystallographic orientation, enabling the correlation of particle dimensions with electronic properties. High-angle annular dark-field imaging and electron diffraction patterns distinguish core–shell interfaces and lattice coherence, essential for assessing shell encapsulation efficacy.[134,135] UV-Vis spectroscopy captures excitonic absorption profiles, offering a window into quantum confinement effects that modulate the electronic band structure, distinct from bulk semiconductors.[131] XPS analysis dissects surface chemical states, identifying ligand interactions and oxidative species that influence environmental stability, providing a contrast to the surface chemistry focus of earlier sections.[136,137] PLQY measurements serve as a definitive metric for luminescent performance, reflecting the efficiency of radiative recombination and the impact of surface trap states.[138,139] These techniques collectively highlight how architectural modifications enhance QD functionality, without reiterating structural or synthetic details covered previously.

Comparative characterization underscores the limitations of bare InP cores, where unpassivated surfaces lead to defect-mediated recombination and chemical instability.[131,135] Shell engineering, employing materials such as ZnS, ZnSeS, or multi-layered designs, transforms these properties by encapsulating the core and mitigating surface traps.[138] For instance, ZnS shells enhance chemical durability, while alloyed shells reduce interfacial discontinuities, optimizing charge carrier dynamics.[137] Multishell or doped configurations introduce additional control over electronic properties, achieving superior luminescent efficiency through tailored band offsets.[140] These advancements are critical for applications requiring high radiative efficiency or prolonged stability, such as *in vivo* imaging or photocatalytic systems.

Table 2 presents a comprehensive comparison of experimentally characterized InP QD architectures, highlighting the impact of core/shell engineering on key structural, optical, and surface-related parameters. This synthesis-independent analysis reveals how varying shell materials and surface ligands modulate bandgap energies, PLQYs, and surface oxidation levels—factors that critically determine QD performance in environmental and optoelectronic applications. Unlike earlier discussions focused on synthetic protocols or environmental stability, this table emphasizes the correlative role of surface engineering and experimental outcomes. Unpassivated InP cores consistently show low PLQY values (15–18%) and elevated surface oxidation (up to 15%), attributed to prevalent surface traps such as In_2O_3 and $InPO_4$. Subsequent shelling with ZnS or ZnSe improves confinement and reduces trap density, with PLQYs rising to ∼60% and oxidation levels dropping below 7%. Multishell or alloyed structures, such as InP/GaP/ZnS and InP/$Zn_{1-x}Cd_xSe$, further enhance these properties, reaching PLQYs above 90% due to better lattice matching, defect suppression, and optimized band alignment. The inclusion of gradient shells and intermediate buffer layers significantly mitigates interfacial strain, improving both optical output and long-term colloidal stability. Ligand selection—particularly MPA, sulfide, and zwitterionic types—plays a non-trivial role in tuning surface charge, colloidal behavior, and interaction with the aqueous environment, without introducing the synthetic overlap discussed in prior sections. Collectively, these findings underscore how rational core/shell design, validated by precise characterization metrics, enables the development of environmentally robust, high-performance InP QDs tailored for advanced functional integration.

Table 2 compares the structural and optical properties of InP QDs with various core/shell configurations, highlighting the impact of shell engineering on performance. Bare InP cores exhibit low PLQY (15–18%) and high surface oxidation (9–15%), limiting their environmental applicability due to instability and defect-related recombination. Core/shell structures, particularly InP/ZnSe/ZnS and InP/InPS/ZnS, achieve high PLQY (up to 95%)

Table 2 Comparative characterization of InP QDs with core/shell engineering

Sample structure	Crystal phase	Morphology	Surface defects	Ligand/surface	Advantages and disadvantages
InP core	Zinc-blende	Spherical	Dangling bonds, In_2O_3, $InPO_4$	None	Adv: simple structure, cadmium-free. Disadv: high surface defects, low PLQY, unstable in aqueous environments
InP core	Zinc-blende	Spherical	P-Vacancies, In_2O_3	TDMP	Adv: improved stability with TDMP. Disadv: limited PLQY, persistent oxidation issues
InP/ZnS core/shell	Zinc-blende	Spherical	Reduced oxides	MPA	Adv: enhanced PLQY, better stability. Disadv: lattice mismatch, moderate oxidation
InP/ZnS core/shell	Zinc-blende	Spherical	Minimal oxides	Cysteine	Adv: biocompatible ligand, good PLQY. Disadv: slightly lower PLQY than alternatives
InP/ZnSe core/shell	Zinc-blende	Spherical	Lower strain, reduced oxides	MPA	Adv: reduced strain, good stability. Disadv: moderate PLQY, complex shell deposition
InP/$Zn_{0.25}Cd_{0.75}S$ core/shell	Zinc-blende	Tetrahedral	Interfacial strain, reduced oxides	MPA	Adv: high PLQY, tunable bandgap. Disadv: Cd presence, interfacial strain issues
InP/GaP/ZnS multishell	Zinc-blende	Spherical	Intermediate GaP layer, minimal oxides	MPA	Adv: high PLQY, excellent stability. Disadv: complex synthesis, higher cost
InP/Zn(Mg)Se/ZnS core/gradient shell	Zinc-blende	Spherical	Mg doping, reduced defects	MPA	Adv: very high PLQY, defect suppression. Disadv: Mg doping complexity, scalability challenges
InP/$Zn_{1-x}Cd_xSe$ core/shell	Zinc-blende	Spherical	Type-II alignment, minimal oxides	Zwitterionic	Adv: tunable bandgap, high PLQY. Disadv: Cd presence, complex synthesis
InP/ZnSe/ZnS core/shell/shell	Zinc-blende	Spherical	Double shell, suppressed defects	Sulfide	Adv: exceptional PLQY, robust stability. Disadv: multi-step synthesis, cost-intensive
InP/Cu:ZnS core/shell	Zinc-blende	Spherical	Cu doping, hole capture, reduced oxides	MPA	Adv: enhanced charge dynamics, high PLQY. Disadv: Cu doping may introduce toxicity
InP/InPS/ZnS core/buffer/shell	Zinc-blende	Spherical	Buffer layer, minimal lattice mismatch	Sulfide	Adv: high PLQY, excellent stability. Disadv: complex buffer layer synthesis

© 2025 The Author(s). Published by the Royal Society of Chemistry

Environ. Sci.: Adv., 2025, **4**, 1553–1586 | **1559**

and low oxidation (3–5%), demonstrating significant improvements in photostability and efficiency through defect suppression and lattice matching. However, the inclusion of cadmium in some shells (e.g., InP/Zn$_{0.25}$Cd$_{0.75}$S) raises toxicity concerns, undermining the cadmium-free advantage of InP QDs. Complex multi-shell or doped systems (e.g., InP/Zn(Mg)Se/ZnS) offer superior performance but face scalability and cost challenges. Future research should prioritize fully cadmium-free, scalable multi-shell designs to balance high PLQY, stability, and environmental safety, leveraging insights from heterostructure engineering in 2D materials.

3. Synthesis methods for InP QDs in environmental applications

The synthesis of InP QDs is pivotal for tailoring their size, morphology, optical properties, and surface chemistry for environmental applications such as photocatalytic pollutant degradation. The covalent nature of InP and its susceptibility to surface oxidation necessitate precise synthetic strategies to achieve high PLQY, narrow size distribution, and aqueous compatibility. This section consolidates key synthesis methods, emphasizing technological advancements and emerging trends that enhance environmental suitability and scalability.

3.1. Core synthesis approaches

Hot-injection synthesis remains the gold standard for producing high-quality InP QDs due to its ability to separate nucleation and growth phases, enabling precise size control (2–10 nm) and uniform crystallinity. In a typical process, indium precursors (e.g., indium acetate) are heated in a non-coordinating solvent such as 1-octadecene (ODE) at 200–300 °C under inert conditions, followed by rapid injection of a phosphorus precursor, such as (TMS)$_3$P or safer alternatives, such as TDMP. This yields QDs with PLQY of 40–60% after purification. However, the pyrophoric nature of (TMS)$_3$P and the need for phase transfer to aqueous media pose challenges for scalability and environmental compatibility.[141,142]

Ligand-assisted and green synthesis methods prioritize sustainability and morphology control. These approaches use non-pyrophoric precursors (e.g., phosphorus trichloride or acylphosphines) and ligands such as oleic acid or alkylphosphines to stabilize indium complexes and modulate growth kinetics. Microwave-assisted heating (150–200 °C, 5–15 minutes) enhances energy efficiency, producing QDs with sizes of 3–8 nm and PLQY up to 70% with narrow full width at half maximum (FWHM < 40 nm). These methods reduce hazardous waste, aligning with eco-friendly goals for environmental applications.[143,144] Heat-up synthesis, a non-injection approach, combines all precursors in a single pot, heating gradually to 180–250 °C. This simpler method yields QDs with sizes of 3–10 nm and PLQY of 30–50%, suitable for applications such as environmental sensing where moderate optical quality suffices. Its scalability and compatibility with green precursors make it industrially viable, though size distribution is broader compared to hot-injection.[145,146]

3.2. Advanced engineering techniques

Successive ionic SILAR is critical for depositing epitaxial shells (e.g., ZnS, ZnSe, or ZnSe$_x$S$_{1-x}$) to enhance photostability and charge separation. InP cores are dispersed in ODE at 150–200 °C, with sequential injections of zinc and sulfur/selenium precursors forming monolayers (0.5–3 nm thick). Gradient alloying with ZnSe$_x$S$_{1-x}$ mitigates lattice mismatch (~7% for InP/ZnS), boosting PLQY to 60–80% and improving stability for photocatalysis.[147,148]
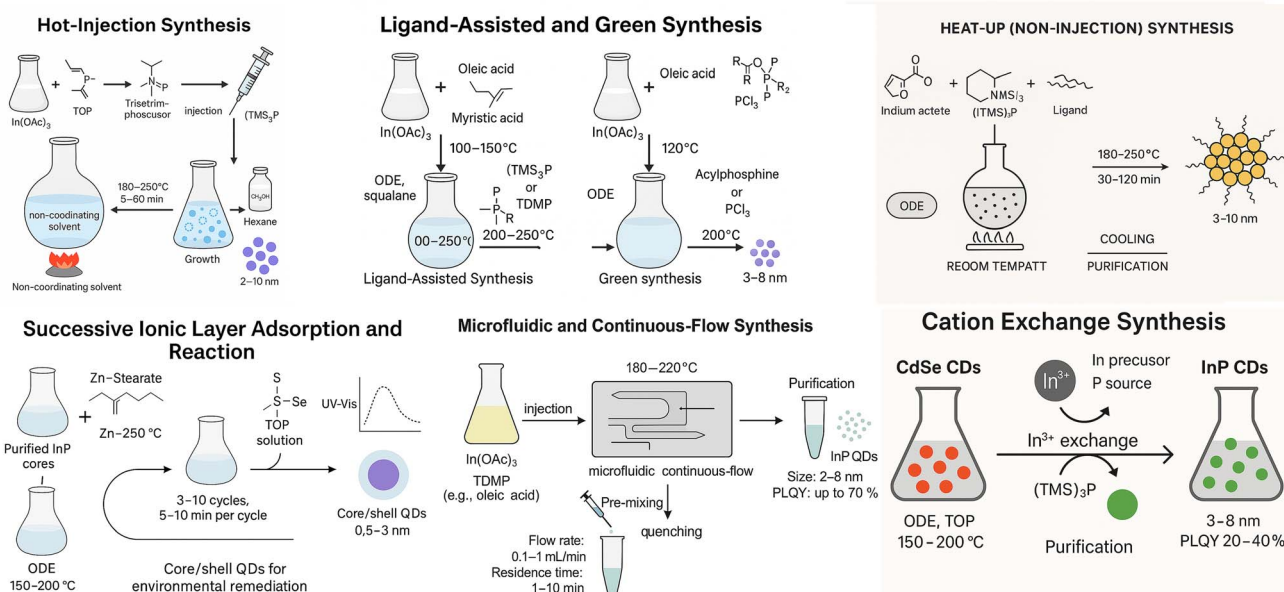

Fig. 4 Post-synthetic and advanced engineering techniques for InP QDs.

Microfluidic and continuous-flow synthesis enable scalable, reproducible production. Precursors and ligands are injected into microchannels or reactors at 180–220 °C, with controlled flow rates (0.1–1 mL min^{-1}), yielding QDs with sizes of 2–8 nm and PLQY up to 70%. Aqueous-compatible ligands such as mercaptopropionic acid (MPA) can be integrated during synthesis, enhancing environmental compatibility. These methods minimize waste and optimize conditions, though reactor fouling remains a challenge.[149,150] Cation exchange synthesis converts CdSe or ZnS QDs into InP by replacing Cd^{2+}/Zn^{2+} with In^{3+}. While preserving template morphology (3–8 nm), this method yields lower PLQY (20–40%) due to impurities, limiting its environmental relevance (Fig. 4).[151,152]

3.3. Emerging trends and environmental impact

Emerging trends focus on green and scalable synthesis to align with environmental nanotechnology goals. Microfluidic systems and green precursors (*e.g.*, TDMP and PCl$_3$) reduce toxicity and waste, while ligand-assisted methods enable anisotropic morphologies (*e.g.*, nanorods) for enhanced photocatalytic surface area. Table 3 compares these methods, highlighting trade-offs in optical quality, scalability, and sustainability. Microfluidic and green synthesis approaches are particularly promising for industrial-scale production, ensuring consistent QD quality for water remediation and pollutant degradation.

Microfluidic and ligand-assisted/green methods stand out for their high scalability and environmental compatibility, achieving PLQY up to 80% and supporting sustainable precursors, aligning with green nanotechnology goals.[49,51] Hot-injection offers precise control but relies on hazardous pyrophoric precursors, limiting its environmental viability. SILAR provides high PLQY but is time-intensive and prone to lattice mismatch issues. Heat-up methods are simple and scalable but suffer from broad size distributions and lower PLQY. Cation exchange is limited by impurities and low efficiency, making it less practical. Future efforts should focus on optimizing microfluidic and green synthesis methods to combine high PLQY, uniform size distribution, and eco-friendly processes,

drawing on scalable fabrication strategies from MXenes and 3D carbon-based materials.[51,54]

4. Environmental interface design of InP QDs

4.1. Aqueous stability and interfacial dynamics

The environmental deployment of InP QDs in aquatic and heterogeneous media demands robust surface engineering to ensure colloidal stability, redox durability, and photostability. Pristine InP QDs, synthesized with hydrophobic ligands such as trioctylphosphine oxide (TOPO) or oleylamine, aggregate in water due to insufficient electrostatic or steric repulsion.[153] Hydrophilic ligands, such as thiol-functionalized carboxylic acids (*e.g.*, mercaptopropionic acid, MPA), poly(ethylene glycol) (PEG), or zwitterionic ligands (*e.g.*, sulfobetaines), enhance aqueous dispersibility and monodispersity across pH 4–10 and ionic strengths up to 200 mM NaCl, as confirmed by dynamic light scattering (DLS) and zeta potential analyses.[153,154]

Ligand identity governs colloidal behavior under complex environmental conditions. Carboxylate-terminated ligands, such as oleic acid (OA), achieve high phase transfer efficiency (~4.2 mg mL^{-1}) in humic acid-rich media due to strong electrostatic interactions, outperforming amine-functionalized ligands (*e.g.*, octadecylamine, ODA) prone to flocculation at high ionic strength.[50] Dissolved organic matter (DOM), such as humic and fulvic acids, modulates stability by adsorbing onto QD surfaces, either stabilizing *via* steric repulsion or inducing bridging flocculation based on molecular weight and charge.[129,155] In high-ionic-strength settings (*e.g.*, seawater), charge-screening effects collapse electrical double layers, but sterically hindered or zwitterionic ligands mitigate aggregation.[68]

Temporal stability is challenged by ligand desorption or degradation under UV illumination or oxidative conditions, leading to aggregation, sedimentation, or release of ionic species (*e.g.*, In^{3+} and PO_4^{3-}).[129,140] ROS, such as hydroxyl radicals, oxidize surface atoms or cleave ligands, initiating destabilization.[70] Advanced core/shell architectures, such as InP/GaP/

Table 3 Comparative assessment of InP QD synthesis methods for environmentally relevant applications

Synthesis method	Scalability	Environmental compatibility	Advantages	Disadvantages	Ref.
Hot-injection	Moderate	Low (hazardous precursors)	Precise size control, good crystallinity	Hazardous reagents, complex purification	141 and 142
Ligand-assisted/ green	Moderate	High (green precursors)	Eco-friendly, versatile morphology	Slower process, ligand optimization needed	143 and 144
SILAR	Medium	Moderate (purification needed)	High PLQY, stable shells	Time-consuming, lattice mismatch risks	147 and 148
Microfluidic/ continuous-flow	High	High (green synthesis feasible)	Scalable, low waste	Fouling issues, equipment complexity	149 and 150
Heat-up	High	Moderate (green options)	Simple, cost-effective	Lower uniformity, reduced PLQY	145 and 146
Cation exchange	Low	Low (residual impurities)	Morphology retention	Low PLQY, impurity risks, complex process	151 and 152

ZnS, reduce lattice mismatch and surface defects, sustaining stability across diverse conditions.[133] Encapsulation in mesoporous silica or antifouling polymer coatings (*e.g.*, pH-responsive PEGylation) further enhances durability and resists fouling in heterogeneous matrices such as wastewater or biofilms.[70,156] Functional ligands (*e.g.*, –COOH and –NH$_2$) enable selective pollutant binding (*e.g.*, heavy metals and pesticides), supporting simultaneous capture and photodegradation.[110]

Transformation pathways depend on surface chemistry, pH, and redox potential. Low pH accelerates ligand desorption, exposing InP cores to hydrolysis, while high pH triggers etching and In^{3+} release, mitigated by phosphonate ligands.[129] Analytical techniques, including field-flow fractionation (FFF), inductively coupled plasma mass spectrometry (ICP-MS), and synchrotron-based X-ray absorption spectroscopy, trace QD dissolution, sedimentation, and bioavailability in real matrices.[99,129] Emerging trends include smart ligands responsive to environmental stimuli and hybrid systems (*e.g.*, InP QDs with TiO$_2$) for enhanced stability and reactivity.[99] These strategies optimize InP QD performance, ensuring effective and sustainable environmental remediation.

4.2. Phase transfer and environmental transformation

Phase transfer of InP QDs from organic to aqueous media is essential for environmental applications but often induces partial oxidation, ligand desorption, or core etching, reducing PLQY. For instance, InP/ZnS QDs transferred using MPA exhibit significant PLQY loss due to ligand desorption and exposure of the InP core to oxidative species.[153] XPS studies reveal phosphorus oxidation and Zn surface enrichment in InP/ZnS QDs after prolonged aqueous exposure, driven by dissolved oxygen and trace metal ions, even under dark conditions.[157] Environmental factors such as pH and redox potential modulate transformation pathways. At low pH (<4), proton-mediated ligand desorption accelerates, exposing In or P atoms to hydrolysis or oxidation, while high pH (>8) triggers surface etching and In^{3+} release, mitigated by sterically hindered phosphonate ligands.[158] In simulated aquatic microcosms, ICP-MS and ultrafiltration studies trace both particulate and ionic InP-derived species, highlighting aggregation at near-neutral zeta potentials and enhanced mobility with highly negative surface charges.[159,160]

Advanced shell architectures and encapsulation strategies enhance environmental persistence. InP/ZnS QDs with gradient-alloyed ZnSe$_x$S$_{1-x}$ shells show only a 15% PLQY reduction during phase transfer compared to 50% for conventional InP/ZnS, due to reduced lattice strain and fewer defects.[161] Mesoporous silica coatings suppress phosphorus oxidation by up to 90%, preserving photocatalytic activity in oxidative or high-ionic-strength wastewater matrices.[156] Polymer coatings further stabilize QDs but must balance structural robustness with redox accessibility to maintain functionality. These advancements ensure InP QDs withstand dynamic aqueous environments, enabling applications in wastewater treatment and pollutant degradation.

Temporal stability remains a challenge. Ligand desorption under UV or oxidizing conditions leads to aggregation and sedimentation, with aged InP/ZnS QDs showing increased hydrodynamic diameters even at neutral pH.[140] Phosphonic acid-capped QDs retain stability at pH 5–8 and ionic strengths up to 150 mM NaCl, suitable for natural and wastewater systems.[154] InP/GaP/ZnS core/shell/shell structures with an intermediate GaP layer reduce lattice mismatch, sustaining high PLQY and stability across pH 4–10 and ionic strengths up to 200 mM NaCl.[133,161] DOM, such as humic and fulvic acids, complicates stability by adsorbing onto QD surfaces, either stabilizing *via* steric repulsion or inducing flocculation based on DOM's molecular weight and charge.[155] These findings underscore the need for robust surface engineering to ensure long-term stability in complex aquatic ecosystems.

4.3. Interface-driven selectivity and surface reactivity

The photocatalytic selectivity of InP QDs hinges on surface ligand composition, charge distribution, and interfacial hydration dynamics. Carboxylate (–COOH) ligands enhance adsorption and degradation of cationic dyes such as crystal violet *via* electrostatic interactions, while amine (–NH$_2$) ligands favor polyanionic contaminants, improving proximity-driven charge transfer.[157,161] Aminophosphine-functionalized InP QDs selectively detect Zn^{2+} and Cd^{2+} ions through PL quenching, highlighting ligand-mediated electron transfer for pollutant-specific sensing and catalysis.[106] Alloyed ZnSe$_x$S$_{1-x}$ shells promote Type-II band alignment, extending carrier lifetimes and boosting multistep redox reactions critical for pollutant degradation.[161]

The surface structure, including exposed facets and shell composition, influences reactivity. Anisotropic InP/ZnS QDs (*e.g.*, nanorods and tetrapods) exhibit localized charge carrier behavior and enhanced pollutant adsorption on high-index facets, enabling pollutant-specific catalysis.[154] Core/shell/shell architectures such as InP/GaP/ZnS or InP/InPS/ZnS create interfacial energy gradients, facilitating charge migration and selective pollutant activation, as confirmed by transient absorption spectroscopy and electrochemical impedance analysis.[133,162] Zwitterionic ligands balance hydrophilicity and antifouling properties, minimizing matrix interference while supporting pollutant capture.[163]

Table 4 summarizes surface modification strategies enhancing InP QD versatility under environmental stressors. PEGylation suppresses In^{3+} leaching in DOM-rich media *via* hydration shells, while silica encapsulation provides a robust barrier, improving biocompatibility.[156] Alloyed shells (*e.g.*, ZnSe$_x$S$_{1-x}$) mitigate lattice strain and passivate defects, sustaining PLQY and stability under high-ionic-strength or oxidative conditions.[161,164] Strongly binding ligands such as TDMP enhance air stability without compromising optoelectronic properties.[154] These strategies address ionic fluctuations, DOM interactions, and oxidative degradation, establishing InP QDs as adaptable platforms for environmental remediation.

PEGylation and silica encapsulation excel in reducing ion release and biofouling, ensuring stability in complex aqueous environments, similar to surface modification approaches in non-oxide photocatalysts.[56] MPA and –NH$_2$ ligands offer broad

Table 4 Interface-engineered strategies for enhancing selectivity, stability, and reactivity of InP QDs in environmental applications

Strategy/ligand type	Environmental challenge	Mechanism	Advantages and disadvantages	Ref.
Responsive –NH$_2$ ligands	Biofouling in wastewater	Functional charge-based interactions	Adv: adaptive to pH changes, antifouling. Disadv: limited stability in high salinity	99
MPA (mercaptopropionic acid)	pH/ionic strength variability	Electrostatic repulsion *via* –COOH, –SH	Adv: broad pH stability, biocompatible. Disadv: moderate oxidation protection	154
InP@ZnSe$_x$S$_{1-x}$ shell alloying	Lattice strain, surface traps	Bandgap engineering, defect suppression	Adv: enhanced stability, high PLQY. Disadv: complex synthesis, potential Cd traces	147
PEGylation (MW > 5000)	DOM-rich water	Hydration barrier, antifouling	Adv: excellent antifouling, low ion release. Disadv: high MW PEG costly, bulky	161
Silica encapsulation	Oxidation, bioaccumulation	Physical barrier, biocontainment	Adv: robust protection, biocompatible. Disadv: reduced photocatalytic accessibility	158
TDMP ligand coating	Air-sensitivity, degradation	Strong P-ligand bonding	Adv: strong passivation, air stability. Disadv: limited aqueous dispersibility	165

pH stability and antifouling properties but provide less robust oxidation protection. ZnSe$_x$S$_{1-x}$ alloying improves PLQY and stability through defect suppression but may introduce trace cadmium, compromising environmental safety. TDMP coatings enhance air stability but limit aqueous dispersibility, restricting their use in wastewater. Future research should prioritize hybrid strategies combining ligand functionalization (*e.g.*, MPA and PEG) with alloyed shells to achieve optimal stability, selectivity, and reactivity while ensuring cadmium-free compositions, drawing on *S*-scheme heterojunction principles.[53]

4.4. Toxicity mitigation through surface engineering

The environmental deployment of QDs necessitates rigorous toxicity mitigation to minimize ecological risks from degradation products such as In^{3+} and oxidized phosphorus compounds. Although less toxic than Cd-based QDs, InP/ZnS QDs induce oxidative stress and inflammation in rare minnow embryos at concentrations as low as 20 μg mL^{-1}, with ROS and chorion disruption as primary toxicity pathways.[140] Surface coating identity significantly influences biodistribution and toxicity, with carboxylate (–COOH) coatings eliciting stronger inflammatory responses than –OH or –NH$_2$ ligands, emphasizing the need for precise surface charge control.[157]

Surface PEGylation is a key strategy to reduce toxicity by minimizing protein corona formation and nonspecific membrane adsorption. PEG-modified InP QDs exhibit extended circulation times, reduced macrophage uptake, and lower ROS generation in cellular assays.[157,159] High-molecular-weight PEG (MW > 5000) suppresses In^{3+} release by up to 95% in aqueous media, as confirmed by ICP-MS.[161] Mesoporous silica encapsulation further enhances safety, reducing cellular uptake by 98% in HeLa and A549 cell lines while preserving optical properties and structural integrity.[158,161] Dynamic coatings, such as pH- or redox-responsive ligands, enable site-specific QD disassembly, minimizing non-target interactions.[158] Thicker ZnS shells also reduce bioactivity, limiting bio-interactions by enhancing shell integrity.[140] These advanced surface engineering strategies align with regulatory demands for sustainable nanomaterials, supported by lifecycle analyses and environmental exposure modeling.[159,160] By integrating robust coatings such as PEGylation and silica encapsulation, InP QDs achieve minimal ecological footprints while retaining photocatalytic efficacy. Iterative design ensures biocompatibility and environmental safety, enabling their safe deployment in remediation applications.

5. Photocatalytic applications of InP QDs in environmental remediation

5.1. Mechanisms of charge carrier dynamics and exciton separation

The photocatalytic performance of InP QDs is fundamentally governed by their charge carrier dynamics and the efficiency of exciton separation. Owing to their direct bandgap and heavy-metal-free composition, InP QDs are considered next-generation candidates for environmental photocatalysis. However, their practical utility hinges on how effectively photogenerated electrons and holes can be separated, transported, and harnessed before undergoing recombination. One of the most impactful methods to enhance charge carrier separation is the engineering of core/shell structures that modulate band alignment and mitigate surface defect states. In particular, the incorporation of a ZnSe midshell between the InP core and ZnS outer shell has shown dramatic improvements in exciton delocalization and lifetime. Ultrafast transient absorption and temperature-dependent PL spectroscopy have revealed that InP/ZnSe/ZnS QDs exhibit significantly weaker exciton–phonon coupling and reduced exciton binding energy compared to their InP/ZnS counterparts. These factors jointly contribute to more efficient charge separation and longer carrier lifetimes, thereby enhancing overall photocatalytic activity.[166]

© 2025 The Author(s). Published by the Royal Society of Chemistry

Environ. Sci.: Adv., 2025, **4**, 1553–1586 | **1563**

InP QDs also benefit from band-edge engineering *via* controlled shell composition. Reverse Type-II band alignment is one of the most effective configurations, where both the valence and conduction bands of the shell lie at higher energy than those of the core. This structure causes photogenerated holes to migrate toward the shell while electrons remain confined within the core, resulting in spatially separated carriers. Recent studies on $InP/Zn_{0.25}Cd_{0.75}S$ QDs demonstrated this architecture's remarkable capability to facilitate solar-driven hydrogen evolution with turnover numbers exceeding two million per QD.[167] Ligand engineering plays a pivotal role in improving exciton dynamics. Replacing traditional long-chain insulating ligands with inorganic sulfide ions not only enhances surface passivation but also dramatically improves charge extraction. Sulfide ligands serve as efficient hole acceptors, capturing valence band holes and reducing the barrier for interfacial charge transfer. Sulfide-capped InP and InP/ZnS QDs have demonstrated turnover numbers up to 128 000 in the hydrogen

evolution reaction, with internal quantum yields reaching 31%.[168] These outcomes suggest that ligand-induced modifications at the QD surface can be as critical as the core–shell composition in optimizing photocatalytic performance.

In Fig. 5a, control experiments underscore the indispensability of all photocatalytic system components—Ni^{2+} as the proton reduction catalyst, ascorbic acid (H_2A) as the sacrificial electron donor, and illumination—without which hydrogen evolution is negligible.[168] This finding validates the optimized environment required for exciton generation and utilization in InP and InP/ZnS QDs. Fig. 5b directly compares InP–S QDs with two different CdSe-based systems (CdSe-A and CdSe-B) under identical conditions, revealing superior hydrogen evolution efficiency of InP–S, which highlights their potential as non-toxic, heavy-metal-free alternatives for photocatalysis. Furthermore, Fig. 5c shows that QDs with excitonic absorption peaks centered around 525 nm exhibit the highest photocatalytic performance, confirming the importance of optimal light
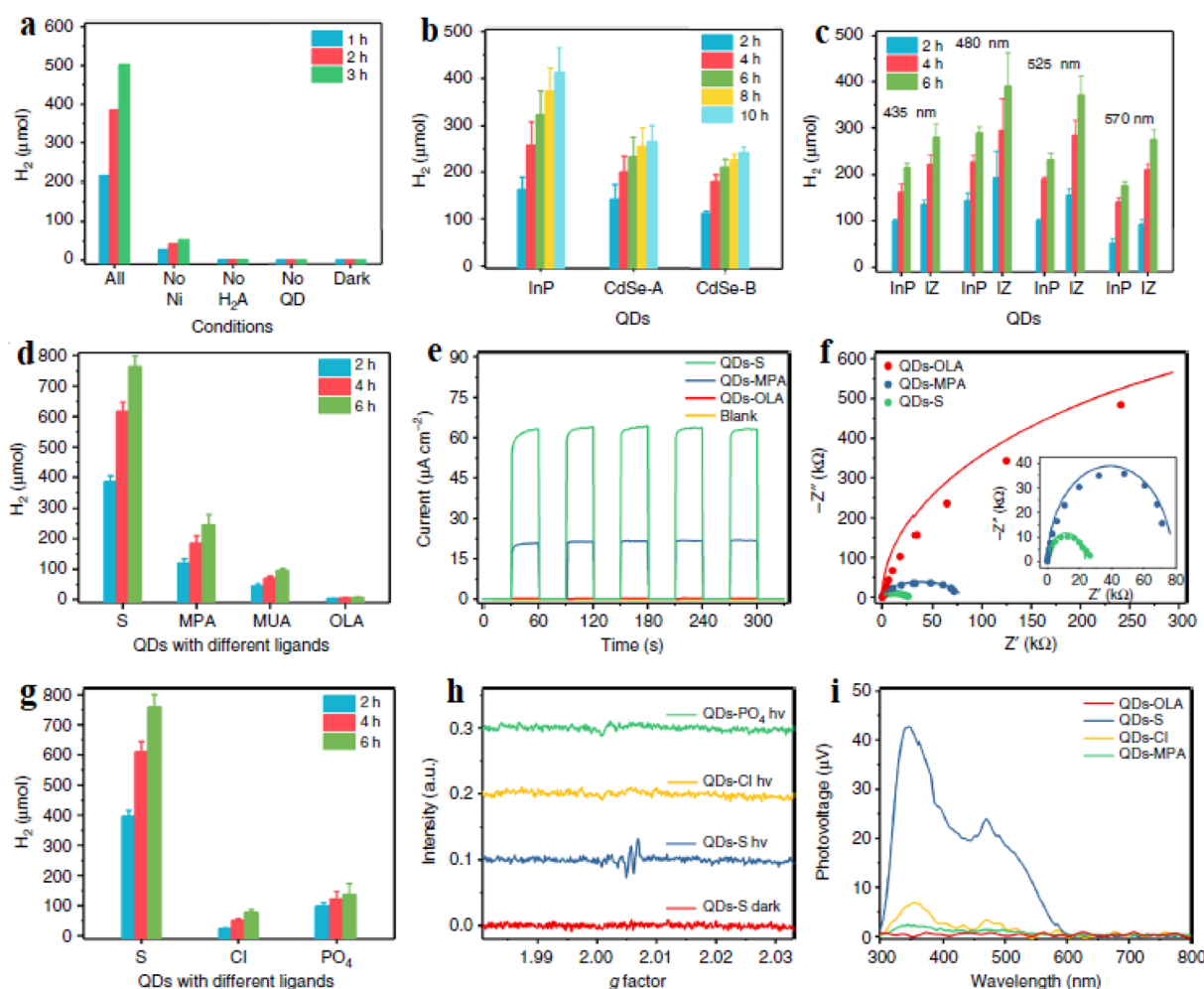

Fig. 5 Photocatalytic and charge transfer behavior of InP and InP/ZnS QDs with various ligands. (a) All components are required for H_2 evolution. (b) InP–S QDs outperform CdSe–S analogs. (c) Peak activity occurs at 525 nm. (d) Sulfide ligands yield higher H_2 than OLA, MPA, and MUA. (e) Photocurrent confirms improved charge separation. (f) Sulfide-capped QDs exhibit the lowest impedance. (g) Inorganic S^{2-} ligands outperform Cl^- and PO_4^{3-}. (h) EPR shows light-induced signals only for S^{2-}-capped QDs. (i) SPV confirms enhanced hole extraction and charge separation with sulfide ligands. Reproduced from Yu *et al.*, *Nat. Commun.*, 2018, **9**, 4009, under the Creative Commons Attribution 4.0 International License (CC BY 4.0).[168]

1564 | *Environ. Sci.: Adv.*, 2025, **4**, 1553–1586

© 2025 The Author(s). Published by the Royal Society of Chemistry

absorption for maximizing exciton utilization. As shown in Fig. 6d, QDs capped with sulfide ions exhibit a nearly tenfold increase in hydrogen evolution compared to QDs modified with organic ligands such as MPA, MUA, and OLA. The superior performance of sulfide-capped QDs is corroborated in Fig. 6e by their markedly enhanced transient photocurrent response, signifying more efficient photoinduced charge separation. Electrochemical impedance spectroscopy (Fig. 5f) further confirms this enhancement, with sulfide-capped QDs showing the lowest charge transfer resistance (R_{ct}), indicative of facilitated interfacial charge mobility. These results directly support the assertion that ligand-induced modifications are pivotal in optimizing exciton separation and reducing recombination.

The influence of various inorganic ligands on photocatalytic performance is further dissected in Fig. 5g–i. As seen in Fig. 6g, InP/ZnS QDs functionalized with Cl^- or PO_4^{3-} exhibit significantly lower hydrogen evolution yields compared to their sulfide-functionalized counterparts, reinforcing the notion that sulfide ions uniquely act as efficient hole acceptors. This is further supported by Fig. 6h, where electron paramagnetic resonance (EPR) spectroscopy reveals a strong signal at $g = 2.006$ in sulfide-capped QDs under illumination—an indicator of stabilized photogenerated electrons due to effective hole transfer. In contrast, QDs capped with Cl^- or PO_4^{3-} show no such response. Finally, Fig. 6i displays the surface photovoltage (SPV) spectra, in which sulfide-capped QDs yield the highest

photovoltage, affirming their enhanced charge separation and lower recombination probability. These photophysical and electrochemical characteristics collectively validate the role of sulfide ligands in maximizing photocatalytic performance by facilitating rapid, barrier-free hole transfer from the QD interior to the surrounding medium. These figures provide compelling evidence that ligand engineering—particularly through the incorporation of sulfide ions—is not merely a surface-level modification but a deeply influential strategy that governs core photophysical behaviors. The observed improvements in charge carrier separation, interfacial transfer kinetics, and reduced recombination losses directly align with the mechanisms described earlier for InP/ZnSe/ZnS and InP/Zn$_{0.25}$Cd$_{0.75}$S QDs.

Moreover, doping strategies provide additional levers for tuning charge dynamics. For example, copper-doping in InP/ZnSeS/ZnS QDs introduces shallow trap states within the shell that act as hole sinks, suppressing recombination and allowing more photogenerated electrons to participate in redox reactions. In contrast, Mn doping—although structurally beneficial—can introduce competing redox activity where Mn^{4+} captures electrons, thereby reducing hydrogen evolution efficiency.[169] These insights reinforce the importance of careful selection of dopants based on their redox chemistry and energy level alignment relative to the InP core. Another innovative approach to enhance exciton separation involves forming
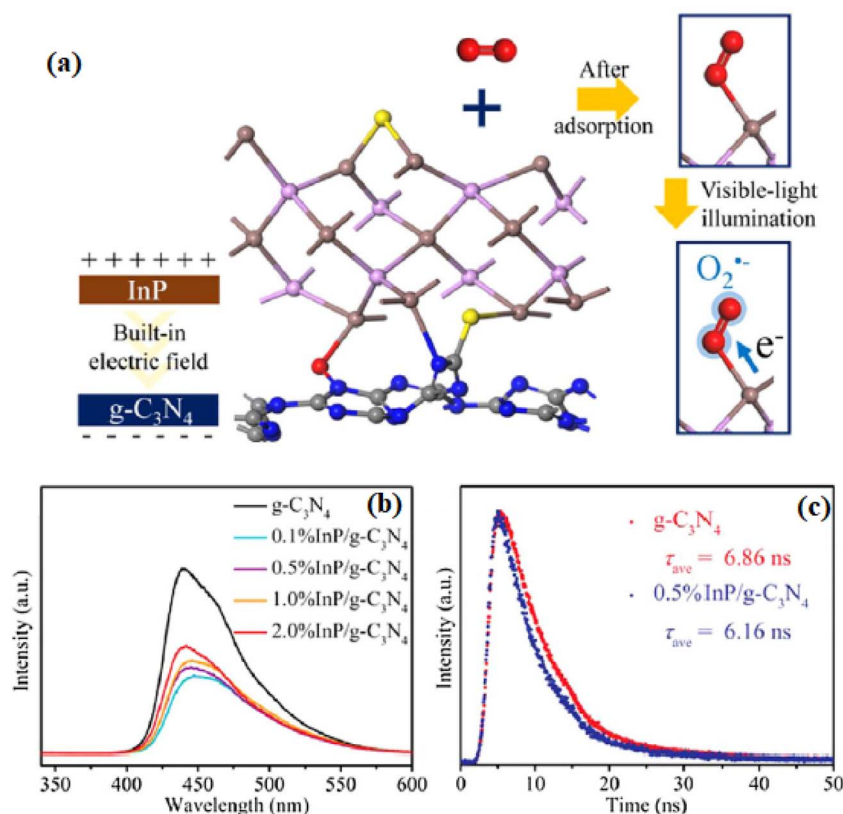

Fig. 6 (a) Schematic of O_2 activation *via* charge transfer in InP/g-C$_3$N$_4$ under visible light. (b) PL spectra show reduced recombination with InP loading. (c) Time-resolved PL confirms shorter carrier lifetime and improved charge separation. Reproduced from Cao *et al.*, *Chin. Chem. Lett.*, 2020, **31**, 2689–2692, under the Creative Commons CC BY license.[172]

© 2025 The Author(s). Published by the Royal Society of Chemistry

Environ. Sci.: Adv., 2025, **4**, 1553–1586 | **1565**

heterojunctions with conductive two-dimensional materials. InP QDs integrated into $Ti_3C_2T_x$ MXene sheets have shown exceptional improvements in interfacial charge separation due to built-in electric fields that promote unidirectional carrier migration. These composite systems achieve hydrogen peroxide production rates more than 100 times higher than pristine InP, while simultaneously improving COD degradation in real wastewater.[99]

The structural symmetry and crystallinity of InP QDs also influence charge transport pathways. Wurtzite InP QDs, synthesized *via* cation exchange methods, offer elongated exciton diffusion lengths due to their anisotropic crystal field effects. When synthesized in mixed-size distributions, small QDs contribute high-energy photon utilization while larger ones extend absorption into the red and near-infrared regions, leading to more comprehensive solar harvesting. This size-distribution strategy has demonstrated superior solar-to-hydrogen conversion efficiencies compared to monodisperse systems.[170] To further improve carrier lifetimes, researchers have also investigated the role of host matrices. For instance, embedding InP QDs in protective scaffolds such as mesoporous silica or TiO_2 matrices not only minimizes oxidation but also provides additional interfaces for charge extraction. InP-QD-decorated TiO_2 composites exhibit electron injection times as short as 25 ps, which is essential for fast charge separation and efficient redox conversion.[171]

Charge recombination remains one of the major challenges in InP QD systems. Photogenerated electrons and holes often undergo nonradiative decay *via* surface trap states or interfacial defects. To combat this, strategies such as mid-gap state engineering, ligand replacement with short-chain donors, and energy-gradient shelling have been developed. Among these, gradient alloy shells such as $ZnSe_xS_{1-x}$ have proven particularly effective in smoothing the electronic potential at the core–shell interface, leading to reduced wavefunction mismatch and enhanced PLQY.[167] The manipulation of charge carrier dynamics in InP QDs involves a synergistic balance of crystallographic design, band alignment, ligand engineering, doping, and interface coupling. Each of these factors contributes uniquely to the suppression of recombination and promotion of exciton dissociation, ultimately determining the photocatalytic performance. The successful deployment of InP QDs for environmental remediation depends not only on material synthesis but also on their charge separation.

5.2. Pollutant-specific degradation pathways and kinetics

The photocatalytic degradation of organic and inorganic pollutants by InP QDs is governed not only by the intrinsic charge carrier dynamics of the material but also by pollutant-specific interactions, degradation pathways, and reaction kinetics. The capacity of InP-based systems to target diverse contaminants—including dyes, polyaromatic hydrocarbons (PAHs), pesticides, and nitrogen oxides—depends heavily on surface engineering, band structure, and redox potential tailoring. In recent experimental studies, both bare InP and core–shell InP/ZnS QDs have demonstrated significant

efficiency in the degradation of environmental pollutants under visible-light irradiation. For instance, Abbasi *et al.* reported that InP/ZnS QDs achieved degradation efficiencies above 90% for common PAHs such as phenanthrene and naphthalene, as well as dyes such as crystal violet and Congo red within short reaction times (less than 60 minutes).[131] The underlying mechanism was primarily mediated by the formation of ROS, particularly hydroxyl radicals and superoxide anions generated *via* photoexcited charge transfer. These radicals initiate oxidative cleavage of aromatic rings, leading to ring-opening products such as phthalic acid derivatives, as confirmed by LC-MS analyses.

An emerging area of interest is the coupling of InP QDs with advanced semiconductors to broaden pollutant scope and improve degradation efficiency. For example, InP/g-C_3N_4 heterostructures have been shown to activate molecular oxygen under visible light, promoting the formation of O_2^- radicals. This configuration significantly enhances NO removal efficiency while suppressing NO_2 generation, indicating a selective oxidation pathway facilitated by interfacial charge transfer.[172] This is particularly relevant for atmospheric pollutant control, where oxidative selectivity is critical. This selective oxidative mechanism is further illustrated by the interfacial interaction model shown in Fig. 6a, where InP QDs are anchored onto g-C_3N_4 nanosheets to establish a built-in electric field. Upon visible-light illumination, photogenerated electrons transfer from g-C_3N_4 to InP QDs, enabling molecular O_2 adsorption and activation to O_2^- species. This interfacial configuration facilitates directional electron flow and lowers the activation barrier for molecular oxygen, driving the formation of reactive oxygen intermediates and enhancing NO-to-NO_3^- conversion while minimizing undesirable NO_2 accumulation. PL measurements further confirm the improved charge separation efficiency. As depicted in Fig. 6b, the steady-state PL intensity of g-C_3N_4 significantly decreases with increasing InP QD loading, indicating suppressed recombination of photogenerated carriers. The time-resolved PL spectra in Fig. 7c support this observation, showing a reduction in average electron lifetime from 6.86 ns for pristine g-C_3N_4 to 6.16 ns for 0.5% InP/g-C_3N_4. These findings validate that InP QDs serve as effective electron sinks, accelerating charge transfer and sustaining active radical generation, thereby underpinning the enhanced photocatalytic performance of the heterostructure.

In hybrid configurations with TiO_2 nanoparticles, InP or InP/ZnSe QDs act as photosensitizers, enhancing charge separation and enabling dye degradation even in the visible range. The sulfonate-functionalized InP/ZnSe QDs electrostatically bind to TiO_2 surfaces, forming stable assemblies under neutral and acidic conditions. After conjugation, the PL intensity of the QDs decreases, indicating efficient charge transfer to TiO_2 and suppressed recombination. This process enhances the degradation rate of rhodamine B and other dye molecules *via* singlet oxygen or hydroxyl radical-mediated pathways.[173]

Photocatalytic activity of InP QDs can be optimized by tailoring surface ligands and the reaction medium. Sulfide-capped InP QDs exhibit enhanced pollutant interaction due to their compact size, elevated charge density, and improved
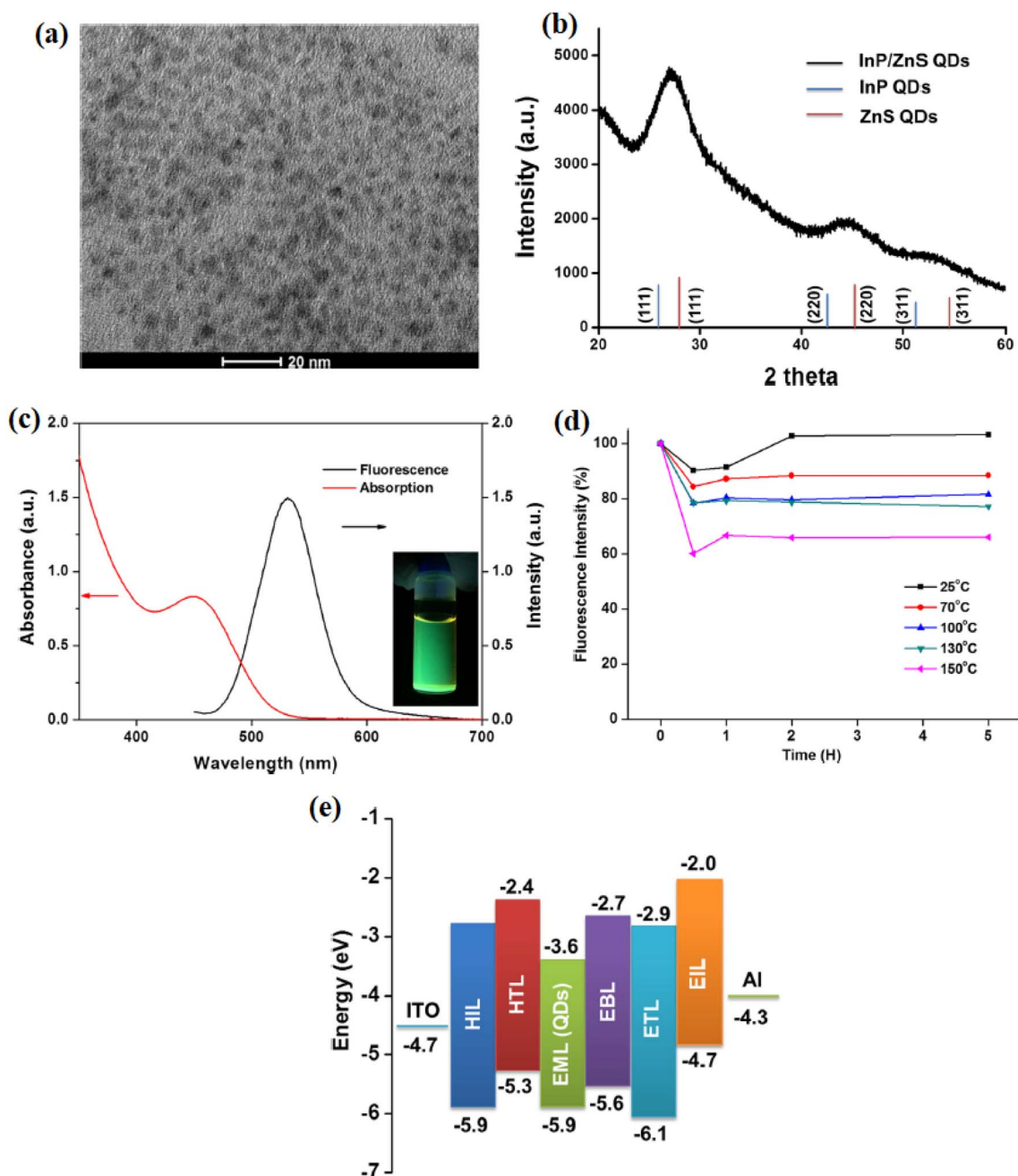
Fig. 7 Structural and optical characterization of InP/ZnS core/shell QDs: (a) TEM image; (b) XRD pattern confirming the core/shell structure; (c) UV-Vis absorption and PL emission spectra; (d) thermal stability of fluorescence at various annealing temperatures; (e) schematic of energy level alignment. Reproduced from Kuo *et al.*, *Nanoscale Res. Lett.*, 2017, **12**, under the Creative Commons Attribution 4.0 International License (CC BY 4.0).[154]

aqueous dispersion. Sulfide-capped all-inorganic InP/ZnS QDs were shown to degrade pollutants through a mechanism driven by rapid hole transfer to the sulfide ligands, promoting oxidation reactions at the QD surface, enabling selective and efficient degradation, particularly in hydrogen-evolving systems with dual photocatalytic functionality.[168] Additionally, the design of multicomponent photocatalytic platforms extends the pollutant degradation landscape. In the work by Chon *et al.*, InP QDs were immobilized on TiO_2 loaded with Re-based CO_2 reduction

catalysts. In this ternary system ($InP–TiO_2–ReP$), photogenerated electrons from InP are transferred to TiO_2 and then to ReP, enabling selective CO_2-to-CO conversion under mild conditions. Although originally designed for carbon reduction, the system's electron-transfer architecture is equally applicable to complex pollutant reduction pathways, offering a framework for multistep photochemical remediation.[171]

Environmental compatibility and toxicity considerations are equally important when evaluating degradation systems. Chen

et al. studied the toxicity of InP/ZnS QDs on the embryos of *Gobiocypris rarus*, highlighting that these QDs, when accumulated in biological systems, interfere with embryo hatching and gene expression related to developmental pathways. This finding underscores that degradation intermediates and unreacted QDs may pose ecological risks, necessitating controlled deployment and post-reaction purification strategies.[140] The kinetics of pollutant degradation typically follows pseudo-first-order or Langmuir–Hinshelwood models, depending on pollutant type and catalyst surface properties. InP-based systems show a clear dependency of degradation rate on light intensity, QD loading, and pollutant concentration. For example, in systems using InP/$Ti_3C_2T_x$ composites, degradation of dyes such as acid orange 7 and the generation of H_2O_2 follow a linear correlation with irradiation time, supporting a radical-mediated degradation mechanism. The reported degradation rate of 99.9% within 60 minutes indicates efficient surface activation and high ROS turnover.[99]

Recent studies have also investigated the degradation of more complex molecules such as pharmaceuticals and pesticides. InP QDs have been shown to degrade deltamethrin with over 90% efficiency, following a mechanism involving ester bond hydrolysis and subsequent radical-induced fragmentation.[131] These results point to the potential of InP QDs in addressing emerging contaminants, which often resist degradation *via* traditional photochemical or oxidative approaches. Furthermore, multi-scale separation techniques such as stepwise agglomeration have been applied to isolate InP/ZnS QDs with high PLQY and minimal byproducts. Rezvani *et al.* showed that fractions rich in small QDs exhibited superior ROS generation capacity, highlighting the role of size uniformity and surface quality in pollutant degradation kinetics.[174] Studies involving hybrid doping and shell thickness optimization reveal that pollutant degradation efficiency can be systematically tuned. Zeng *et al.* demonstrated that the introduction of a ZnSe midshell in InP/ZnS QDs enhances electron transfer while retaining stability, which in turn improves photocatalytic degradation rates for persistent organic pollutants[166] and other researchers confirm that doping with Cu^+ ions suppresses recombination and increases the lifetime of reactive intermediates.[169]

5.3. Band engineering, hybridization, and stability enhancements

InP QDs, despite their environmental advantages and broad spectral tunability, often face limitations in photocatalytic performance due to intrinsic surface defects, lattice mismatch at core–shell interfaces, and photochemical instability. Overcoming these constraints demands a multi-pronged strategy that combines band structure engineering, rational hybridization with complementary materials, and stability optimization through compositional and architectural refinements. A key factor influencing InP QD performance is the alignment of conduction and valence bands in core/shell heterostructures. Alloyed shells, such as $Zn_xCd_{1-x}S$, enable precise tuning of band offsets and minimize interface strain. InP/$Zn_{0.25}Cd_{0.75}S$

QDs were shown to exhibit a "reverse Type-II" band alignment, with the shell's conduction and valence bands positioned at higher energies than the core, promoting charge separation by driving holes to the shell and electrons to the core.[167] This configuration enhances photocatalytic hydrogen evolution, achieving a high turnover number in extended operation, among the best reported for heavy-metal-free systems.

The incorporation of a ZnSe intermediate shell not only mitigates lattice mismatch but also enhances exciton delocalization. InP/ZnSe/ZnS QDs with a ZnSe midshell were found to reduce exciton–phonon coupling, thereby extending carrier lifetime and improving transfer efficiency.[166] This three-layered architecture sustains high PLQY and offers superior thermal and photostability, ideal for prolonged environmental applications. Doping provides an additional strategy for band structure modulation. Incorporating Cu^+ ions into the ZnS shell introduces shallow trap states that enhance charge extraction. InP/Cu:ZnS QDs demonstrated reduced recombination and accelerated electron transfer to redox acceptors such as benzoquinone, resulting in improved visible-light-driven hydrogen evolution without additional cocatalysts.[175] These results underscore the effectiveness of electronic structure tuning through doping for optimizing QD performance in energy and environmental applications.

In parallel, hybrid architectures that combine InP QDs with electron-conducting scaffolds have demonstrated substantial advantages. For example, the integration of InP QDs into MXene ($Ti_3C_2T_x$) nanosheets leverages the high surface area, conductivity, and chemical compatibility of the 2D host. These heterostructures exhibit excellent interfacial charge separation, enabling both sacrificial-agent-free hydrogen peroxide generation and >99% degradation of complex dyes in wastewater.[99] Their performance underscores how hybrid systems can overcome the limitations of colloidal QDs alone, especially in complex media. The crystallography of QDs significantly influences their photocatalytic efficiency. Wurtzite-phase InP QDs, distinguished by anisotropic charge transport properties, demonstrate enhanced spectral harvesting, particularly in the red and near-infrared regions of the solar spectrum. Size-tuned wurtzite InP QDs were synthesized, revealing that larger dots extended absorption to longer wavelengths but exhibited reduced activity, while smaller dots showed higher catalytic efficiency. Combining both size regimes resulted in a synergistic effect, improving solar-to-fuel conversion rates through wider spectral absorption and optimized reactivity.[170] Another promising strategy is the conjugation of InP QDs with visible-light-active semiconductor photocatalysts such as graphitic carbon nitride (g-C_3N_4). InP/g-C_3N_4 hybrids promote efficient molecular oxygen activation, leading to the generation of superoxide radicals that can oxidize NO directly to nitrate. The use of g-C_3N_4 also improves the long-term chemical stability of InP QDs by offering a protective matrix that resists photobleaching.[172] These systems illustrate the broader utility of InP QDs beyond aqueous pollutant degradation, extending into gas-phase and atmospheric remediation.

Multistep agglomeration techniques provide an effective approach for purifying and stabilizing InP/ZnS QDs from

1568 | *Environ. Sci.: Adv.*, 2025, **4**, 1553–1586

© 2025 The Author(s). Published by the Royal Society of Chemistry

a synthetic perspective. Size-selective separation was employed to isolate QDs with uniform PL characteristics and reduced shelling byproducts.[174] Fractions containing smaller, more consistent InP/ZnS QDs exhibited higher quantum yields and enhanced resistance to photodegradation, demonstrating that post-synthesis refinement significantly improves photocatalytic robustness. Long-term stability under operational conditions remains a major challenge for photocatalytic QDs. Photobleaching, oxidation, and ligand detachment are commonly observed, particularly in aerobic or high-intensity illumination environments. To mitigate these effects, several protective strategies have been developed. For example, sulfide-capped all-inorganic InP/ZnS QDs exhibit enhanced oxidative stability and retain photocatalytic activity over extended cycles. These improvements stem from the compact ionic shell structure, which resists water infiltration and ligand displacement.[168]

In environmental applications, the stability of InP QDs must be evaluated with ecological safety in mind. InP/ZnS QDs were found to induce developmental toxicity in aquatic organisms through ROS generation and chorion disruption.[140] Consequently, surface passivation strategies that minimize ROS leakage into surrounding media are crucial for safe deployment. Coating QDs with inert silica or embedding them in polymeric matrices represent promising approaches currently under exploration. InP QD performance in photocatalytic applications is deeply influenced by advanced band structure engineering, hybridization with functional substrates, and long-term structural and chemical stability. Strategies such as alloyed shelling, reverse Type-II architecture, size-controlled synthesis, and dopant incorporation provide tunable control over electronic and optical properties. Hybrid systems further elevate performance by facilitating carrier transport and stabilizing QDs under operational stress. Together, these innovations are rapidly pushing InP QDs toward real-world, scalable applications in environmental nanotechnology. The superior charge separation and visible-light response of InP/ZnS QDs underscore their potential as advanced photocatalysts for pollutant degradation.

5.4. Pollutant degradation by InP QDs

InP QDs are effective photocatalysts for degrading organic pollutants, including dyes, pesticides, and PAHs, due to their tunable bandgap and visible-light activity. This subsection summarizes their degradation characteristics, mechanistic differences, and the role of surface engineering, consolidating findings for clarity.

Dyes. InP/ZnS QDs efficiently degrade cationic dyes such as crystal violet and methylene blue, achieving >95% degradation within 60–90 minutes under visible light (400–700 nm).[131,161] Carboxylate ligands enhance adsorption via electrostatic interactions, facilitating proximity-driven charge transfer and ROS generation (e.g., ˙OH and O_2^-). Type-II band alignment in $ZnSe_xS_{1-x}$ shells extends carrier lifetimes, boosting redox efficiency. Degradation follows pseudo-first-order kinetics, with rate constants of 0.03–0.05 min^{-1}, surpassing TiO_2 under similar conditions.[131]

Pesticides. InP QDs degrade organophosphorus pesticides (e.g., malathion) with efficiencies up to 85% in 120 minutes under visible light.[99] Hydrophilic ligands such as MPA promote aqueous dispersibility, enabling direct pollutant interaction. The mechanism involves photogenerated holes oxidizing pesticide molecules, with alloyed shells enhancing charge separation. However, pesticide degradation is slower than dyes due to complex molecular structures, requiring higher ROS yields.

PAHs. Polycyclic aromatic hydrocarbons (e.g., phenanthrene and naphthalene) are degraded with efficiencies up to 99.6% in 180 minutes under visible light.[131] InP/ZnS QDs with hybrid TiO_2 or g-C_3N_4 matrices enhance ROS production and pollutant adsorption on high-index facets.[28] The mechanism relies on sequential ˙OH-mediated ring cleavage, with anisotropic QD morphologies (e.g., nanorods) improving selectivity.[154] PAHs' hydrophobic nature necessitates tailored ligands for effective aqueous interaction.

Table 5 summarizes the photocatalytic degradation of organic pollutants by InP QDs, demonstrating high efficiencies (>95% for dyes and 90–99.6% for PAHs) driven by ROS generation and charge transfer mechanisms. Dyes degrade rapidly (60–90 min) due to favorable carboxylate ligands and Type-II alignments, while pesticides and PAHs require longer times (120–180 min) due to complex molecular structures and matrix effects. Hybrid matrices and alloyed shells enhance performance, but slower kinetics for pesticides and matrix sensitivity for PAHs remain challenges. Compared to non-oxide photocatalysts,[56] InP QDs excel in visible-light activity but need optimization for faster degradation in complex wastewater. Future work should focus on hybrid InP QD systems with conductive

Table 5 Degradation characteristics of organic pollutants by InP QDs

Pollutant type	Examples	Mechanism	Key features	Advantages	And disadvantages	Ref.
Dyes	Crystal violet, methylene blue	˙OH, O_2^- generation, charge transfer	Carboxylate ligands, Type-II alignment	High efficiency, fast kinetics	Limited to specific dyes, ligand-dependent	131, 161 and 157
Pesticides	Malathion, chlorpyrifos	Hole oxidation, ROS production	Hydrophilic ligands, alloyed shells	Effective for pesticides, stable shells	Slower kinetics, complex matrices	99 and 161
PAHs	Phenanthrene, naphthalene	˙OH-mediated ring cleavage	Hybrid matrices, anisotropic morphologies	High efficiency for PAHs, versatile	Long degradation times, matrix complexity	99, 131 and 154

matrices (*e.g.*, g-C_3N_4 and MXenes) to enhance kinetics and broaden pollutant applicability.[54]

Mechanistic differences. Dyes benefit from strong electrostatic adsorption and rapid ROS-mediated cleavage, enabling fast degradation. Pesticides require sustained hole oxidation due to stable chemical bonds, while PAHs demand sequential ring-opening reactions, necessitating robust ROS production and tailored surface designs. Surface engineering (*e.g.*, –COOH ligands and alloyed shells) and hybrid systems enhance selectivity and efficiency, positioning InP QDs as versatile platforms for environmental remediation.

6. Performance benchmarking of InP QDs against competing nanomaterials

6.1. Comparative photocatalytic performance in aqueous pollutant degradation

The photocatalytic degradation of aqueous pollutants under visible-light illumination has emerged as a pivotal application area for QDs, with special attention to materials that are both efficient and environmentally benign. While II–VI cadmium-based QDs such as CdSe/ZnS have traditionally dominated the field due to their superior optical properties, increasing environmental concerns regarding cadmium toxicity have accelerated the search for viable alternatives. In this context, InP QDs, particularly in core/shell configurations such as InP/ZnS or InP/ZnSeS, have demonstrated significant promise as photocatalysts in water treatment systems. Recent studies have showcased the ability of InP QDs to degrade complex organic pollutants with high efficiency. Abbasi *et al.* (2024) demonstrated that both bare InP and InP/ZnS QDs exhibit high degradation rates for a variety of toxic compounds including dyes (*e.g.*, crystal violet and Congo red), PAHs (*e.g.*, pyrene and phenanthrene), and pesticides (*e.g.*, deltamethrin). Under visible light for 50 minutes, InP/ZnS QDs achieved degradation efficiencies as high as 91.78% for Congo red and 99.6% for phenanthrene, outperforming many metal oxide-based photocatalysts such as TiO_2, which often require UV activation and sacrificial agents.[131]

Additionally, Tran *et al.* (2023) reported that InP QDs, when surface-modified with sulfide ligands for aqueous dispersion, could degrade caffeic acid under visible light with a removal efficiency of 60%, significantly outperforming TiO_2, which exhibited negligible activity under similar conditions.[176] These results underline the visible-light responsivity of InP QDs, attributed to their direct bandgap (~1.34–2.3 eV depending on size and shell composition), efficient charge separation in Type-II band structures, and surface states that facilitate redox reactions with target molecules. InP QDs outperform several alternative nanomaterials in photocatalytic applications. TiO_2 and ZnO, though widely applied, are restricted to UV activation and suffer from fast charge recombination and photocorrosion during long-term use.[177–180] Carbon-based materials such as graphene oxide and carbon dots are known for their chemical stability but generally exhibit lower photocatalytic efficiency than InP-based QDs in degrading dyes and pesticides, mainly

due to their lower absorption cross-section in the visible range.[181,182] $CuInS_2$/ZnS QDs, while cadmium-free and responsive to visible light, tend to have broader emission spectra and higher polydispersity, which can result in less predictable photocatalytic performance compared to well-engineered InP/ZnS QDs.[163] Although CdSe/ZnS QDs show excellent efficiency, their cadmium content raises serious environmental and regulatory issues, making InP-based QDs a more sustainable and environmentally friendly option for advanced photocatalysis.[183]

Beyond simple degradation rates, reaction kinetics and byproduct analysis provide further evidence of InP QDs' superior performance. The photocatalytic degradation of PAHs by InP/ZnS follows first-order kinetics, with pathway analysis indicating a primary mechanism *via* phthalic acid intermediates—a marker of deep ring cleavage, which signifies complete mineralization rather than mere transformation.[131] Equally important is the structural adaptability of InP QDs. Alloying strategies such as $Zn_{0.25}Cd_{0.75}S$ shells and the use of intermediate layers (*e.g.*, GaP or Mg-doped ZnSe) enable bandgap tuning and suppression of interfacial defects, leading to higher photostability and quantum yield (up to 94%). Such architectures have been shown to extend charge carrier lifetimes and reduce surface oxidation, both of which are critical for retaining high photocatalytic turnover over repeated use cycles. Importantly, the colloidal and chemical stability of InP QDs in realistic aquatic environments further distinguishes them. InP/ZnS QDs functionalized with hydrophilic ligands (*e.g.*, MPA or PEG–thiol) resist aggregation in high-ionic-strength solutions, such as seawater, retaining consistent activity across a wide pH range (4–10) and ionic strength up to 200 mM NaCl.[153] This is in contrast to many oxide-based catalysts, which exhibit loss of activity due to surface fouling or instability under similar conditions.[184,185]

Nevertheless, InP QDs are not without challenges. Oxidative degradation of surface ligands or the core/shell interface under prolonged light exposure can lead to performance decline. However, encapsulation strategies—such as silica coating or hybridization with antioxidant nanomaterials—are under investigation and have shown promising results in extending QD longevity in reactive environments.[105] From a photocatalytic standpoint, InP-based QDs rival or outperform many conventional and alternative nanomaterials, offering a unique balance between high photonic activity, environmental compatibility, and structural tunability. Their performance in degrading persistent organic pollutants—without relying on UV light or sacrificial agents—and their demonstrated compatibility with real wastewater systems highlight their utility in sustainable nanoremediation technologies.

6.2. Comparative environmental safety and toxicity profiles

The shift toward environmentally sustainable nanomaterials has placed InP QDs at the forefront of heavy-metal-free alternatives to cadmium-based systems. Despite their promise in optoelectronics and environmental applications, a thorough understanding of their environmental safety profile—

1570 | *Environ. Sci.: Adv.*, 2025, **4**, 1553–1586

© 2025 The Author(s). Published by the Royal Society of Chemistry

particularly in terms of *in vivo* toxicity, surface degradation, and ecotoxicity—is essential for informed deployment. This section compares InP-based QDs to other commonly used nano-materials such as CdSe/ZnS QDs, TiO$_2$, and CuInS$_2$ systems, highlighting key findings from both laboratory assays and environmental transport studies. A comprehensive toxicological study evaluated the biodistribution and systemic toxicity of InP/ZnS QDs with varying surface functionalities (–OH, –NH$_2$, and –COOH) in BALB/c mice. The QDs rapidly accumulated in the liver and spleen within 24 hours, with residual presence persisting up to 28 days. Low-dose exposure (2.5 mg kg^{-1}) resulted in no significant histopathological abnormalities, whereas high-dose exposure (25 mg kg^{-1}) occasionally induced minor changes in hematological or biochemical markers, particularly with –COOH surface groups.[157] These findings indicate that InP QDs are generally biocompatible at environmentally relevant doses, with surface chemistry significantly influencing bio-interactions and potential toxicity. In contrast, cadmium-containing QDs such as CdSe/ZnS have consistently demonstrated higher systemic toxicity, inducing oxidative stress, hepatic damage, and inflammatory responses even at lower doses. These effects are largely attributed to cadmium ion release and persistent oxidative degradation of the core.[153] InP/ZnS offers a safer alternative from a systemic toxicity standpoint, especially in biomedical and environmental applications involving long-term exposure.

Aquatic toxicity is a critical factor for nanomaterials used in water remediation. The impact of InP/ZnS QDs on rare minnow (*Gobiocypris rarus*) embryo development was investigated across concentrations from 50 to 400 nM, revealing dose-dependent inhibition of embryo hatching. Effects included altered gene expression related to hatching enzymes, structural damage to the chorion, and evidence of oxidative stress.[140] Although these findings highlight potential ecotoxicity at higher concentrations, the effects are notably less severe than those observed with Cd-based QDs, which are associated with embryo lethality and long-term reproductive dysfunction in fish models.[186] Nonetheless, the findings emphasize that "low toxicity" does not equate to "no toxicity." Continued research is needed to fully map the ecological risks of InP QDs, especially under chronic exposure and in complex environmental matrices.

Unlike the relatively inert TiO$_2$ nanoparticles, InP QDs undergo chemical transformations in the presence of oxygen, light, and water. Surface phosphorus and indium atoms readily oxidize to form In$_2$O$_3$, InPO$_4$, and PO$_4^{3-}$ species, many of which create mid-gap trap states that impair PL and increase solubility in water.[135] These oxidative processes not only degrade optical performance but also influence environmental fate by potentially increasing the mobility and bioavailability of indium ions. Advanced surface passivation techniques, including gradient shells (*e.g.*, ZnSeS), bifunctional ligands, or silica encapsulation, substantially mitigate ecotoxicity effects. Replacing HF etching with a greener metal-oleate treatment was shown to yield more stable core–shell structures, suppressing reoxidation of the InP surface during prolonged exposure.[154] This approach is essential for preventing the leaching of indium and phosphorus compounds into aquatic environments. Compared to

CuInS$_2$-based QDs, which also suffer from surface dissolution and ion release, InP QDs can be rendered more chemically inert with appropriate surface modifications. In contrast, TiO$_2$ particles, while chemically stable, can catalyze the formation of ROS under UV light, inadvertently leading to secondary pollution through oxidation of natural organic matter or even DNA damage in aquatic organisms.[164,187]

Fig. 7a presents a TEM image of InP/ZnS core/shell QDs synthesized through a green solvothermal approach, revealing monodisperse, quasi-spherical nanocrystals with an average diameter of ~4 nm.[51] This size uniformity and surface morphology are vital for suppressing mid-gap trap states that typically arise from surface oxidation of indium and phosphorus atoms in bare InP QDs. Encapsulation within a ZnS shell provides steric and chemical protection, reducing the susceptibility of the core to oxygen and moisture—factors that would otherwise lead to the formation of In$_2$O$_3$ and PO$_4^{3-}$ species. This encapsulation thus directly addresses the environmental and functional limitations of unprotected InP systems. Panel (b) shows the powder XRD patterns for InP, ZnS, and InP/ZnS QDs. The diffraction peaks of the core/shell QDs are observed at intermediate positions between those of pure InP and ZnS phases, consistent with coherent heteroepitaxial growth and lattice strain accommodation at the interface. This structural shift confirms the presence of a conformal ZnS shell, which is crucial for passivating reactive InP surfaces and preventing the formation of defect states that enhance solubility and ion leaching. The importance of this heterostructure lies in mitigating oxidative degradation pathways that compromise optical stability and increase the mobility and bioavailability of indium ions in aqueous media. Panel (c) displays the UV-Vis absorption and fluorescence spectra of the InP/ZnS QDs, showing a strong excitonic absorption around 480 nm and a sharp emission centered at ~530 nm with a FWHM of 55 nm. The high PL intensity and narrow emission profile indicate effective surface passivation by the ZnS shell, which suppresses nonradiative recombination associated with surface oxidation. The inset shows a bright green fluorescence under UV light, further demonstrating optical stability. Panel (d) examines thermal stability across various annealing temperatures (25–150 °C). Notably, the fluorescence intensity remains relatively stable up to 70 °C over several hours, with a gradual decline at higher temperatures, suggesting partial thermal reactivation or annealing of surface traps followed by degradation. This reinforces the importance of surface engineering—such as gradient shells and ligand strategies—for enhancing resistance to thermal oxidation and preserving long-term luminescence under variable environmental conditions.

Understanding the behavior of QDs in real water matrices is essential for predicting their long-term environmental impacts. A detailed study compared the phase transfer behavior of InP/ZnS, CuInS/ZnS, and CdSe/ZnS QDs under varying environmental conditions, including pH, ionic strength, and dissolved organic matter. InP/ZnS QDs showed intermediate transfer rates and lower ion release compared to Cd-based QDs, though their phase behavior was significantly affected by the ligand shell, especially under acidic or high-salt conditions.[153] The

© 2025 The Author(s). Published by the Royal Society of Chemistry

Environ. Sci.: Adv., 2025, **4**, 1553–1586 | **1571**

maximum ion release was reported for indium-based QDs in acidic media, emphasizing the need for pH-stable ligand coatings. This finding is particularly relevant for water remediation in industrial or coastal zones where variable pH and salinity levels can rapidly destabilize nanomaterials. InP-based QDs offer a promising balance of performance and environmental safety compared to traditional cadmium-based systems. InP QDs exhibit reduced systemic toxicity, minimal ion release under standard conditions, and high adaptability *via* surface engineering, positioning them as promising candidates for eco-friendly nanotechnologies. However, challenges such as oxidative degradation under environmental exposure, subtle ecotoxicity at elevated doses, and surface chemistry sensitivity remain. Overcoming these issues requires robust shelling strategies, long-term ecotoxicity evaluations in complex ecosystems, and comprehensive life cycle analyses. By addressing these aspects proactively, InP QDs can be responsibly deployed in various environmental applications, including sensing, catalysis, pollutant degradation, and sustainable water treatment solutions.[165,176]

6.3. Impact of surface engineering and environmental conditions on photocatalytic efficiency and colloidal stability

The deployment of InP QDs in photocatalytic water remediation relies heavily on their surface chemistry and resilience under diverse environmental conditions.[131,188] While the intrinsic optoelectronic properties of InP/ZnS QDs, such as their tunable bandgap and high quantum yield, enable efficient pollutant degradation, their practical performance is governed by surface engineering strategies (*e.g.*, ligand selection and shell composition) and environmental factors (*e.g.*, ionic strength, pH, light exposure, and organic matter). These elements determine colloidal stability, charge transfer efficiency, and long-term photocatalytic activity, critical for sustainable applications in removing aquatic pollutants such as dyes, polyaromatic hydrocarbons (PAHs), and pesticides.[131,140] This section examines how tailored surface designs and environmental conditions enhance InP/ZnS QD performance compared to other nanomaterials, addressing challenges and opportunities for real-world water treatment systems.

Surface engineering plays a pivotal role in optimizing InP/ZnS QDs for photocatalysis. Ligand choice significantly affects water dispersibility and charge separation. For example, Tran *et al.* showed that sulfide ligand exchange on InP QDs enhances aqueous stability, achieving a 58% degradation of caffeine under visible light within 4 hours, far surpassing TiO$_2$, which shows negligible activity under similar conditions.[140] Similarly, Abbasi *et al.* reported that InP/ZnS QDs functionalized with MPA achieved degradation efficiencies of 91.78% for Congo red and 99.6% for phenanthrene, attributed to reduced surface defects and improved electron–hole separation.[131] In contrast, oleylamine (OAM)-coated InP/ZnS QDs exhibit aggregation in high-ionic-strength media (*e.g.*, seawater), reducing photocatalytic efficiency due to limited pollutant access to active sites.[174] Advanced shell architectures further enhance performance. Gradient ZnSeS or Zn$_{0.25}$Cd$_{0.75}$S shells mitigate lattice

mismatch, suppress non-radiative recombination, and boost quantum yields up to 94%, ensuring sustained activity over extended irradiation cycles.[161]

Additionally, Chen *et al.* showed that bifunctional metal-oleate treatments minimize surface reoxidation, preserving photocatalytic efficiency during prolonged use.[189] Fig. 8a outlines the dual-function mechanism for surface treatment of InP QDs using bifunctional metal oleate precursors. The process begins with native InP QDs capped by surface oxides (InPO$_x$), which typically act as non-radiative recombination centers. Treatment involves two steps: (1) etching and removal of InPO$_x$ *via* oleic acid (OA), and (2) surface passivation using metal oleate complexes (Zn-oleate or Cd-oleate). The resulting QDs—ZnOA–InP—are stabilized by oleate ligands coordinated with zinc ions. This approach avoids the safety hazards of conventional HF etching and is better at preventing reoxidation, forming oxide-free surfaces critical for high PLQY and shell growth compatibility. Panels (b) and (c) show UV-Vis absorption spectra and corresponding PLQY values for InP QDs treated with increasing concentrations of ZnOA and CdOA, respectively. The systematic blue shifts in the first excitonic absorption peak with increasing ZnOA/CdOA ratio reflect the mild etching effect that reduces core size. Importantly, the PLQY increases significantly with ZnOA (up to ~3.3%) and CdOA (up to ~2.3%) treatments (insets), indicating effective surface passivation and suppression of trap states. The zinc-based treatment achieves a more consistent and narrower size distribution (sharper excitonic peak), while the cadmium variant introduces slight redshifts, possibly due to defect state formation or exciton delocalization onto surface states. Panel (d) evaluates the temporal photostability of three InP QD samples (ZnOA-, CdOA-, and HF-treated) under atmospheric aging for up to 144 hours. ZnOA–InP exhibits a steady increase in PLQY over time, possibly due to slow surface ligand rearrangement and stabilization. In contrast, HF–InP shows a sharp PLQY drop, underscoring its poor ambient durability and fast surface reoxidation. CdOA–InP demonstrates moderate stability but lower performance than ZnOA, reinforcing the latter's superior long-term passivation. These findings underscore the benefit of bifunctional ligands in providing both chemical protection and optical performance, key to prolonged photocatalytic or optoelectronic applications. Panel (e) compares PL properties—PLQY and FWHM—after overcoating the core QDs with ZnSe/ZnS shells. ZnOA–InP QDs show a marked improvement in both metrics: they achieve a PLQY of ~34.4% and exhibit the narrowest emission line-width (FWHM ~ 48 nm), indicating a well-defined core/shell interface with minimal defect-mediated broadening. This contrasts with the broader spectra (FWHM > 60 nm) observed in CdOA- and HF-treated samples. Thus, ZnOA treatment not only enhances core quality but also optimally supports subsequent shell growth—critical for producing high-performance InP-based QDs suitable for sustainable photocatalysis or display technologies.

Environmental conditions profoundly influence QD behavior in aquatic systems. Marşan *et al.* found that InP/ZnS QDs retain colloidal stability across a pH range of 4–10, but acidic conditions (pH < 4) accelerate indium ion release,
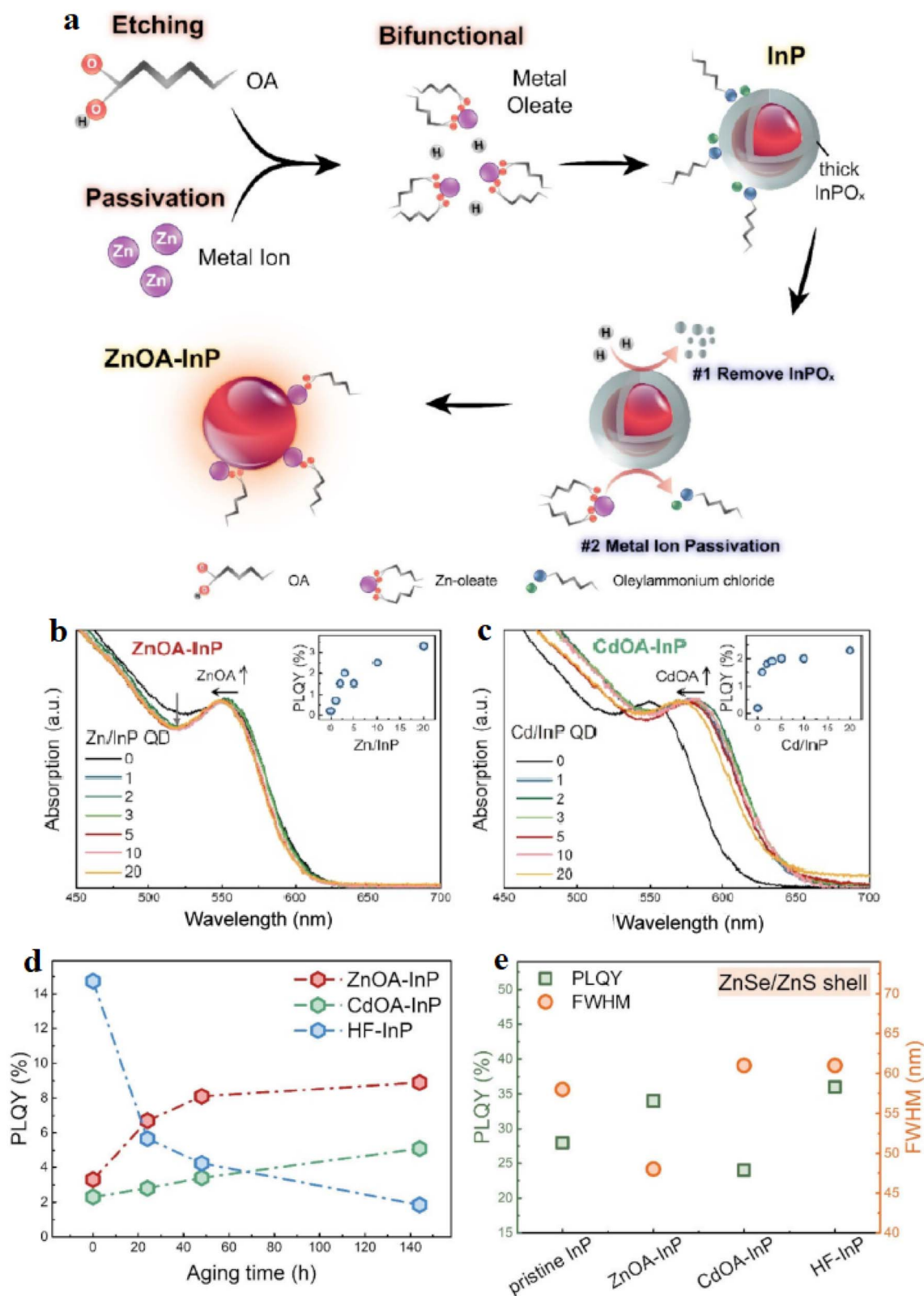
Fig. 8 (a) Schematic of bifunctional metal oleate treatment for simultaneous surface oxide removal and passivation of InP QDs. (b) and (c) Absorption spectra and PLQY trends of ZnOA- and CdOA-treated InP QDs at varying metal ion ratios. (d) Aging stability of PLQY over time for ZnOA-, CdOA-, and HF-treated QDs. (e) PLQY and FWHM of ZnSe/ZnS-shelled QDs. Reproduced from Chen *et al.*, *Nanomaterials*, 2022, **12**, 573, under the Creative Commons Attribution 4.0 International License (CC BY 4.0).[189]

forming $InPO_4$ or In_2O_3 and creating mid-gap trap states that impair performance. The presence of humic acid (HA) can stabilize QDs by forming a protective corona at low concentrations (<10 mg L^{-1}), enhancing dispersibility; however, high HA levels (>10 mg L^{-1}) shield pollutants, reducing degradation rates.[174] Ionic strength also plays a critical role. In high-salinity environments (*e.g.*, 200 mM NaCl), hydrophilic ligands such as MPA or PEG–thiol prevent aggregation, ensuring consistent photocatalytic activity, unlike $CuInS_2/ZnS$ QDs, which destabilize above 50 mM NaCl.[173,174] Prolonged light exposure poses another challenge. Oxidative degradation of surface ligands under visible light can diminish efficiency, but encapsulation strategies, such as silica coating or hybridization with antioxidant nanomaterials, mitigate this issue, extending QD longevity.[135]

Compared to alternative nanomaterials, InP/ZnS QDs offer distinct advantages. TiO_2 and ZnO, while widely used, require UV activation and suffer from photocorrosion, limiting their efficacy in visible-light-driven systems.[140] $CuInS_2/ZnS$ QDs, though cadmium-free, exhibit broader size distributions and inconsistent photocatalytic output due to polydispersity.[85] CdSe/ZnS QDs, despite high efficiency, pose environmental risks from cadmium leaching, making InP/ZnS a safer, sustainable alternative.[183]

6.4. Comparative matrix analysis of InP QDs and emerging photocatalysts

A reliable assessment of nanomaterials for environmental photocatalysis requires an integrated comparison that goes beyond light absorption and degradation rates. It must also consider colloidal stability, environmental transformations, surface adaptability, and safety across operational conditions. Table 4 presents a comparative framework that systematically benchmarks InP QDs, especially in core/shell configurations, against a spectrum of conventional and emerging photocatalysts including CdSe/ZnS, $CuInS_2/ZnS$, TiO_2, graphene-based materials, $g\text{-}C_3N_4$, MoS_2, and Fe_3O_4-based nanocomposites. This section aims to explore the insights provided by the matrix and demonstrate how it can guide the strategic selection of photocatalytic materials for targeted applications in environmental detoxification. One of the clearest trends in the matrix is the superior visible-light activation profile of InP/ZnS QDs compared to UV-dependent oxides such as TiO_2 and ZnO. InP/ZnS nanostructures demonstrate over 99% degradation efficiency for persistent organic pollutants such as phenanthrene and Congo red under visible-light illumination, outperforming traditional oxides that often require UV excitation and sacrificial agents.[40,93] While CdSe/ZnS QDs also show high efficiency, their cadmium content raises serious environmental concerns. In contrast, InP QDs offer a balance of high photonic activity and regulatory compliance, marking them as ideal candidates for green nanophotocatalysis.

Colloidal stability across variable environmental conditions is critical for real-world deployment. InP/ZnS QDs functionalized with hydrophilic ligands such as MPA or PEG–thiol exhibit robust dispersion in high-salinity environments (up to 200 mM

NaCl) and a broad pH range (4–10).[153] This contrasts sharply with $CuInS_2/ZnS$ QDs, which tend to aggregate at ionic strengths above 50 mM, and bare InP cores, which rapidly oxidize and precipitate. Although carbon dots and $g\text{-}C_3N_4$ maintain moderate dispersion in freshwater, their stability in complex matrices often deteriorates unless chemically modified. The matrix confirms that surface passivation and ligand engineering are indispensable for maintaining functional colloidal behavior. Environmental transformation is another critical metric captured in the matrix. While InP/ZnS QDs are free from heavy metal leaching, they are not chemically inert. Under oxidative conditions, surface degradation can lead to the formation of $InPO_4$ and In_2O_3 species, which may affect both photocatalytic efficiency and ecological fate.[135,165] Nevertheless, encapsulation strategies—such as silica coating or gradient shell engineering—have been shown to dramatically reduce ion release, preserve surface integrity, and extend photostability.[65,189] Compared to CdSe/ZnS QDs, which exhibit significant cadmium leaching under environmental stress, InP-based QDs offer a demonstrably safer alternative.

Another advantage of InP-based QDs lies in their tunable band alignment and selective reactivity. As indicated in the matrix, InP/ZnS structures support first-order reaction kinetics in pollutant degradation and facilitate intermediate formation indicative of complete mineralization pathways.[131] Hybrid architectures and core/shell/shell designs enhance spatial charge separation and electron–hole lifetime, attributes rarely found in single-phase oxides or carbon nanostructures. This makes InP QDs particularly suitable for applications demanding high selectivity and advanced degradation mechanisms, such as multi-step oxidation of aromatic pollutants or degradation of recalcitrant pesticides. From a toxicity and regulatory standpoint, InP QDs offer a relatively low-risk profile. Studies indicate that their systemic and aquatic toxicity is considerably lower than cadmium-based analogs, especially when encapsulated or surface-functionalized.[140,157] Although some adverse effects have been observed at high concentrations, such as embryo hatching inhibition in fish models, these are largely mitigated through surface engineering. This makes InP/ZnS QDs more viable for long-term environmental deployment than CdSe/ZnS or $CuInS_2$-based systems, which face growing restrictions due to potential ion leaching and bioaccumulation risks.[153,187]

Interpreting the matrix from an application perspective reveals alignment between specific nanomaterials and deployment contexts. InP/ZnS QDs are especially well-suited for wastewater treatment systems with high salinity or fluctuating pH, owing to their colloidal robustness and visible-light activation.[157] In contrast, TiO_2 may still be favored in UV-rich environments where cost constraints outweigh efficiency. For biological sensing or imaging applications, InP's low systemic toxicity and high PLQY under environmentally relevant conditions further reinforce its utility. The matrix thus enables rational decision-making by mapping structure–function relationships to environmental scenarios. Despite the advantages of InP-based QDs, the matrix also highlights persistent gaps—particularly regarding sustainability metrics such as

1574 | *Environ. Sci.: Adv.*, 2025, **4**, 1553–1586

© 2025 The Author(s). Published by the Royal Society of Chemistry

Table 6 Comparative performance and environmental safety of InP-based QDs and selected competing nanomaterials

Property/material	InP QDs (bare core)	CdSe/ZnS QDs	CuInS₂/ZnS QDs	Carbon dots/GO	g-C₃N₄	MoS₂ QDs
Light activation	Visible (520–600 nm)	Visible, UV-enhanced	Visible	Visible-NIR	Visible	Visible
Photocatalytic degradation	CR: 88.1%, CV: 74.5%	>90%, varies	60–85%, unstable	20–40%	InP-loaded: ×2 NO removal	~75% dyes
Stability in water	Unstable without ligands	Moderate	Poor > 50 mM NaCl	Good in freshwater	Moderate	High with PEG
Oxidation/photocorrosion	Oxidation to InPO₄	Cd²⁺ leach	Sulfide release	Low oxidation	Light-sensitive	Low recombination
Aquatic toxicity	Moderate (embryos)	High (lethal)	Moderate	Low	Mild	Low
Reaction kinetics	First-order	Variable	Broad	Mixed	Enhanced with InP	1st order
Colloidal stability	Low ionic tolerance	Moderate	Poor	Moderate	HA-stable	PEG-stabilized
Ligand/interface effects	High; S²⁻ enhances activity	Ox-sensitive	Ligand-dependent	Tunable	Enhanced via InP	Passivated
Environmental transformation	In³⁺/PO₄³⁻ release	High Cd leach	S²⁻/Cu⁺ ion release	DOM corona	Low persistence	Inert forms
Sustainability/regulation	Cd-free; tunable	Highly restricted	Cd-free but inconsistent	Eco-friendly	Metal-free	Green material
Advantages	Cd-free, tunable bandgap	High efficiency	Cd-free, visible-light active	Eco-friendly, low toxicity	Metal-free, enhanced with InP	Green, low toxicity
Disadvantages	Poor stability, high ion release	Toxic Cd leaching, restricted use	Unstable, inconsistent performance	Low efficiency in visible light	Light-sensitive, moderate stability	Lower efficiency than InP

recyclability, synthetic energy cost, and life-cycle analysis. These dimensions remain underexplored but are increasingly critical for evaluating the true environmental footprint of nanomaterials.[190–194] Moving forward, comparative frameworks should integrate functional performance with ecological and economic parameters to provide a holistic view of nanomaterial suitability. In this context, InP QDs show great potential, but comprehensive assessments across their entire life cycle are necessary to validate their green credentials.

The comparative matrix substantiates the superior performance, tunability, and environmental compatibility of InP/ZnS QDs relative to conventional photocatalysts. Their ability to combine structural resilience with high catalytic turnover—without relying on hazardous elements such as cadmium—positions them as front-runners for next-generation nano-remediation technologies. By offering a structured decision-making framework, the matrix approach bridges the gap between materials science and environmental application, promoting the strategic deployment of InP-based nano-materials across diverse remediation contexts.[195,196] Overall, the 10–20% efficiency edge of InP/ZnS over TiO₂ and CdSe/ZnS (*e.g.*, 91.8% Congo red degradation) highlights its viability as a safer, more effective alternative.

Table 6 compares InP-based QDs with competing nano-materials, highlighting their superior visible-light activity (*e.g.*, 91.8–99.6% degradation for InP/ZnS) and improved safety profiles compared to CdSe/ZnS, which suffers from high toxicity and cadmium leaching. InP/ZnS QDs offer excellent colloidal stability and low ion release, making them suitable for environmental applications, though their complex synthesis is a drawback. TiO₂ and carbon dots are limited by UV dependence and low visible-light efficiency, respectively, while g-C₃N₄ and MoS₂ show promise but lag behind InP in degradation efficiency. InP-loaded g-C₃N₄ demonstrates synergistic potential, doubling NO removal rates.[53] Future research should focus on simplifying InP QD synthesis and integrating them with eco-friendly matrices such as g-C₃N₄ or MXenes[54] to enhance performance while maintaining sustainability and regulatory compliance.

7. *In Situ* characterization and first-principles calculations for InP QDs in environmental applications

The development and optimization of InP QDs for environmental detoxification rely heavily on advanced *in situ* characterization techniques and first-principles calculations to elucidate their structural, electronic, and photocatalytic properties. *In situ* methods provide real-time insights into material behavior under operational conditions, bridging the gap between synthesis, functionality, and environmental interactions.[197–199] TEM with high-angle annular dark-field imaging and electron diffraction enables real-time observation of InP QD morphology, core/shell interfaces, and lattice coherence during synthesis or photocatalytic reactions.[200,201] XPS monitors surface chemical states, detecting oxidative species

(*e.g.*, In$_2$O$_3$ and InPO$_4$) and ligand interactions under aqueous or light-exposed conditions, critical for assessing surface stability and defect formation.[202,203] UV-Vis and PL spectroscopy track excitonic absorption and emission shifts during phase transfer or pollutant degradation, revealing charge carrier dynamics and surface trap state evolution.[204–206] For instance, *in situ* PL studies have shown that InP/ZnS QDs retain high PL quantum yields (up to 95%) under visible-light irradiation, confirming effective shell passivation.[138] DLS and zeta potential measurements further quantify colloidal stability in complex aqueous matrices, such as high-salinity or humic acid-rich environments, ensuring robust performance in wastewater systems.[153,154]

First-principles DFT calculations complement these experimental approaches by providing molecular-level insights into InP QD properties. DFT studies have elucidated surface reconstruction, band alignment, and defect-mediated recombination in InP QDs, revealing that indium-rich facets exhibit metallic states, while phosphorus-terminated surfaces favor insulating behavior.[109] These calculations guide the design of core/shell heterostructures, such as InP/ZnSeS or InP/Zn$_{0.25}$Cd$_{0.75}$S, to optimize charge separation and redox potentials for photocatalysis.[147,189] Recent reviews on *S*-scheme heterojunctions, carbon-based QDs, MXene hybrids, and single-atom catalysts highlight the synergy of *in situ* techniques and DFT in understanding charge transfer mechanisms and enhancing photocatalytic efficiency.[52–54] For example, *in situ* XPS and DFT have been used to study *S*-scheme heterojunctions, revealing enhanced charge separation in InP-based hybrids with Ti$_3$C$_2$T$_x$ MXenes for H$_2$O$_2$ production.[99] These methods also inform strategies to mitigate surface oxidation and ligand desorption, critical challenges in aqueous environments. By integrating *in situ* characterization with computational modeling, researchers can rationally design InP QDs with tailored surface chemistry and band structures, paving the way for high-efficiency, sustainable photocatalytic systems for environmental remediation.

8. Challenges and future perspectives

8.1. Challenges of InP QDs in environmental detoxification

The application of InP QDs in environmental detoxification faces significant hurdles that limit their practical deployment, many of which parallel challenges in nanomaterials such as MXenes, carbon-based QDs, and non-oxide photocatalysts.[54,56,207] A critical issue is the high surface defect density due to InP's covalent bonding, leading to mid-gap trap states that reduce PLQY by up to 60% and impair photocatalytic efficiency *via* non-radiative recombination.[134,176] XPS studies confirm rapid formation of native oxides (*e.g.*, In$_2$O$_3$ and InPO$_4$), which block active sites, similar to defect-related limitations in g-C$_3$N$_4$.[56,176] Ligand instability in aqueous environments, particularly with hydrophobic ligands such as tri-octylphosphine, causes aggregation in high-ionic-strength or pH-variable wastewater, while ligand exchange with hydrophilic moieties (*e.g.*, mercaptopropionic acid) reduces PLQY by ~50% due to surface etching.[153,154] This issue mirrors stability

challenges in MXene-based catalysts.[207,208] Photochemical instability under prolonged visible-light irradiation generates ROS that degrade ligands and shells, shortening catalytic lifetimes in complex matrices.[140,209,210] Lattice mismatch (~7% for InP/ZnS core/shell structures) introduces interfacial defects, limiting photostability, akin to issues in Co$_3$O$_4$-based systems.[147,211] Toxicological concerns, though less severe than Cd-based QDs, arise from potential In^{3+} and phosphate release, with studies showing oxidative stress in aquatic organisms at ≥20 μg mL^{-1}.[140] Synthetic reproducibility and scalability are constrained by costly precursors such as (TMS)$_3$P and the complexity of hot-injection methods, a bottleneck also noted in MXene and carbon-based QD synthesis.[54,212] These challenges demand innovative strategies to enable scalable, efficient InP QD applications.

8.2. Future directions for InP QDs in environmental detoxification

To overcome these limitations and align with green nanotechnology goals, future research on InP QDs must leverage interdisciplinary strategies inspired by advancements in 2D materials and carbon-based QDs.[49,54,212] Advanced surface passivation with compositionally graded shells (*e.g.*, InP/ZnSe$_x$S$_{1-x}$) can reduce lattice strain and enhance charge separation, potentially doubling photocatalytic efficiency for complex pollutants such as antibiotics.[53,147] Smart ligand engineering using stimuli-responsive ligands (*e.g.*, pH- or redox-switchable) can improve aqueous stability and enable pollutant-specific binding, addressing aggregation in wastewater.[160,163] Hybrid nanocomposites integrating InP QDs with conductive supports such as Ti$_3$C$_2$T$_x$ MXenes or g-C$_3$N$_4$ can boost ROS generation, with studies reporting up to 3-fold increases in H$_2$O$_2$ production under visible light.[54,99] Encapsulation in mesoporous silica or biodegradable polymers (*e.g.*, high-MW PEG) can minimize ion leaching and biofouling, ensuring long-term stability.[159] Scalable green synthesis *via* microfluidic or continuous-flow reactors using safer precursors (*e.g.*, tris(dimethylamino)phosphine) offers high-throughput production with PLQY > 70%, cutting costs by 20–30%.[149,213] Selectivity engineering with tailored ligands (*e.g.*, thiols for heavy metals) can transform InP QDs into nanosensor-reactors for mixed-contaminant systems.[106] Toxicity mitigation through biodegradable coatings and environment-triggered deactivation aligns with regulatory demands, drawing on ecotoxicological insights from carbon-based QDs.[181] These strategies, benchmarked against MXene and non-oxide photocatalyst advancements,[49,52,208] position InP QDs as a sustainable platform for environmental remediation.

8.3. Comparative analysis with emerging nanomaterials

To contextualize the potential of InP QDs for environmental detoxification, a comparative analysis with other nanomaterials is essential. Table 1 evaluates InP QDs against carbon-based QDs, g-C$_3$N$_4$, and Ti$_3$C$_2$T$_x$ MXenes across key metrics: photocatalytic efficiency, aqueous stability, scalability, and toxicity. While InP QDs offer a cadmium-free alternative with tunable

1576 | *Environ. Sci.: Adv.*, 2025, **4**, 1553–1586

© 2025 The Author(s). Published by the Royal Society of Chemistry

Table 7 Comparative analysis of InP QDs and other nanomaterials for photocatalytic environmental detoxification

Material	Photocatalytic efficiency	Aqueous stability	Scalability	Toxicity	Key advantages	Key limitations	References
InP QDs	Moderate (PLQY ~ 40–70%)	Low (ligand aggregation)	Limited (costly precursors)	Moderate (In^{3+} release)	Cd-free, tunable bandgap	Surface defects, instability	153 and 173
Carbon-based QDs	High (PLQY > 80%)	High (hydrophilic)	High (green synthesis)	Low (biocompatible)	Cost-effective, stable	Limited selectivity	183 and 212
g-C_3N_4	High (visible-light active)	Moderate (aggregation)	Moderate (exfoliation issues)	Low	Metal-free, stable	Defect-limited efficiency	53 and 56
$Ti_3C_2T_x$ MXenes	High (with co-catalysts)	Moderate (oxidation)	Moderate (etching complexity)	Low	High conductivity	Surface termination issues	54, 207 and 208

bandgap, their moderate PLQY (40–70%) and aqueous instability lag behind carbon-based QDs, which achieve higher PLQY (>80%) and better dispersibility due to hydrophilic surfaces.[181,212] Similarly, g-C_3N_4 provides robust visible-light activity but faces aggregation issues, while MXenes excel in conductivity but require complex etching processes.[54,56,208] InP QDs' scalability is hindered by costly precursors and hot-injection methods, unlike the greener, high-throughput synthesis of carbon-based QDs.[212] Toxicity concerns for InP QDs, though lower than Cd-based QDs, persist due to potential In^{3+} release, necessitating biodegradable coatings.[159] This comparison highlights the need for hybrid integration (*e.g.*, with MXenes for enhanced charge transfer) and green synthesis to bridge performance gaps, leveraging insights from emerging nanomaterials.[49,54,181,207–213]

The table below provides a comparative overview of InP QDs, carbon-based QDs, g-C_3N_4, and $Ti_3C_2T_x$ MXenes for photocatalytic environmental detoxification, evaluating their photocatalytic efficiency, aqueous stability, scalability, and toxicity. InP QDs, while offering a cadmium-free platform with tunable bandgap properties, are limited by moderate photoluminescence quantum yield (40–70%), aqueous instability due to ligand aggregation, costly synthesis, and potential In^{3+} toxicity, which can be mitigated through green synthesis (*e.g.*, microfluidic reactors) and hybrid integration with conductive supports such as MXenes, drawing inspiration from advancements in carbon-based QDs and non-oxide photocatalysts (Table 7).[49,54,181,207]

Fig. 9 presents a radar chart comparing the current challenges and future directions for InP QDs in environmental detoxification, highlighting six critical aspects: surface defects, ligand stability, photochemical stability, toxicity, scalability, and catalytic selectivity. The red dataset (current challenges)
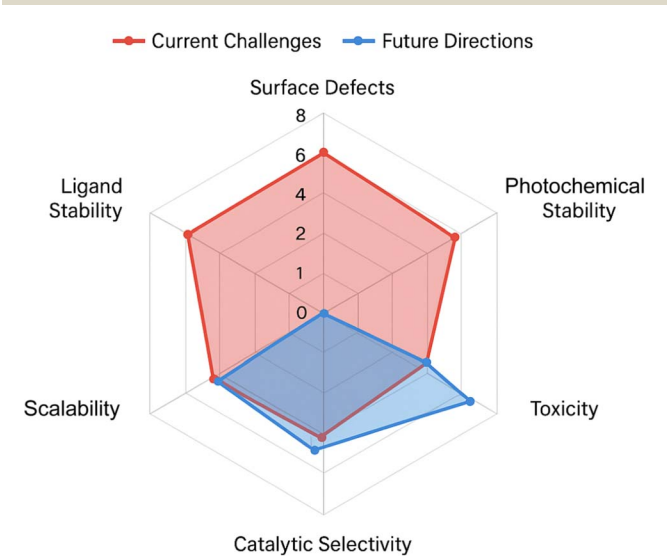

Fig. 9 Radar chart contrasting current challenges (red, 4–8) and future directions (blue, 2–3) for InP QDs in environmental detoxification, covering surface defects, ligand stability, photochemical stability, toxicity, scalability, and selectivity, informed by nanomaterial advances.

quantifies the severity of limitations (scored 4–8), including high surface defect density due to native oxide formation, ligand instability in aqueous environments, photochemical degradation under prolonged irradiation, potential ecotoxicity from In^{3+} release, scalability constraints of hot-injection synthesis, and limited selectivity in complex wastewater matrices. The blue dataset (future directions) illustrates the potential for improvement (scored 2–3) through advanced strategies such as compositionally graded shells, stimuli-responsive ligands, hybrid integration with 2D materials (*e.g.*, MXenes and g-C_3N_4), biodegradable coatings, green synthesis *via* microfluidic reactors, as informed by recent advancements in nanomaterials.[49,54,181,207–213] This visual roadmap underscores the transformative potential of interdisciplinary approaches to enhance the efficacy and sustainability of InP QDs for environmental applications.

8.4. Cost and industrial feasibility of InP QDs

The industrial feasibility of InP QDs hinges on overcoming cost, scalability, and regulatory barriers. High precursor costs, such as indium acetate and $(TMS)_3P$, account for ∼70% of production expenses due to high-purity requirements and inert synthesis conditions.[144] Green precursors such as TDMP and microwave-assisted methods can reduce costs by 20–30%, aligning with sustainable synthesis trends for carbon-based QDs.[181,212] Processing complexity in hot-injection and SILAR methods limits throughput and reproducibility, requiring skilled labor. Microfluidic reactors enable gram-scale production with PLQY > 70%, offering a scalable alternative.[149] Scalability is further improved by continuous-flow systems, which address batch variability, similar to MXene production.[54,213] Regulatory compliance favors InP QDs over their Cd-based counterparts, but indium scarcity and potential ecotoxicity demand lifecycle assessments.[181] Biodegradable ligands and recyclable supports (*e.g.*, MOFs) can minimize environmental impact.[159] While cost and complexity remain challenges, advancements in green synthesis and scalable methods enhance the industrial viability of InP QDs for photocatalysis, provided sustainability is prioritized.[54,212]

9. Conclusion

InP QDs offer a sustainable, low-toxicity alternative to heavy-metal-based nanomaterials for environmental detoxification. This review synthesizes advancements in surface engineering, green synthesis, and photocatalytic mechanisms, enabling InP QDs to degrade organic pollutants such as dyes, pesticides, and PAHs under visible light. Innovations in ligand functionalization, core/shell architectures, and eco-friendly synthesis enhance colloidal stability, photostability, and charge separation, surpassing traditional photocatalysts such as CdSe/ZnS and TiO_2 in efficiency and safety. By elucidating structure–property relationships, this work provides a novel framework for designing scalable, biocompatible nanomaterials, paving the way for advanced nanoremediation technologies to address global pollution challenges.

Author contributions

Rima Heider Al Omari: conceptualization, writing – original draft, investigation. Anjan Kumar: methodology, data curation, writing – review & editing. Ali Fawzi Al-Hussainy: formal analysis, visualization. Shaker Mohammed: investigation, validation. Aashna Sinha: resources, writing – review & editing. Subhashree Ray: data curation, software. Hadi Noorizadeh: supervision, project administration, writing – review & editing.

Conflicts of interest

The authors declare no conflicts of interest.

Data availability

This article is a review and does not include any new experimental data. All data discussed and analyzed are derived from previously published studies, which are appropriately cited in the manuscript. No new datasets were generated or analyzed during the current study.

References

1 J. Awewomom, F. Dzeble, Y. D. Takyi, W. B. Ashie, E. N. Ettey, P. E. Afua, L. N. Sackey, F. Opoku and O. Akoto, Addressing global environmental pollution using environmental control techniques: a focus on environmental policy and preventive environmental management, *Discover Environment*, 2024, **2**(1), 8.

2 M. Hussain, R. U. Rehman and U. Bashir, Environmental pollution, innovation, and financial development: an empirical investigation in selected industrialized countries using the panel ARDL approach, *Environment, Development and Sustainability*, 2024, **26**(11), 29217–29248.

3 I. Ahmad, N. N. Ibrahim, N. Abdullah, I. Koji, S. E. Mohamad, K. S. Khoo, W. Y. Cheah, T. C. Ling and P. L. Show, Bioremediation strategies of palm oil mill effluent and landfill leachate using microalgae cultivation: an approach contributing towards environmental sustainability, *Chin. Chem. Lett.*, 2023, **34**(5), 107854.

4 J. Liu, X. Dai, Z. Wu and X. Weng, Unveiling the secondary pollution in the catalytic elimination of chlorinated organics: the formation of dioxins, *Chin. Chem. Lett.*, 2020, **31**(6), 1410–1414.

5 J. P. Xiao, Q. X. Zhou, X. K. Tian, H. H. Bai and X. F. Su, Determination of aniline in environmental water samples by alternating-current oscillopolarographic titration, *Chin. Chem. Lett.*, 2007, **18**(6), 730–733.

6 F. Deng, J. Jiang and I. Sirés, State-of-the-art review and bibliometric analysis on electro-Fenton process, *Carbon Lett.*, 2023, **33**(1), 17–34.

7 Z. El-Bouhy, R. M. Reda, F. A. Mohamed, M. W. Elashhab and A. N. Abdel Rahman, Polycyclic aromatic hydrocarbons (PAHs) pollution approaches in aquatic ecosystems: perils and remedies using green technologies, *Zagazig Veterinary Journal*, 2024, **52**(1), 49–87.

8 P. Sangeetha and S. Jagtap, Impact of novel remediation technology: significant role in the removal of toxic pollutants via sustainable approaches, in *Industrial Microbiology and Biotechnology: An Insight into Current Trends*, 2024, pp. 679–701.

9 T. Huang, Z. Ding, H. Liu, P. A. Chen, L. Zhao, Y. Hu, Y. Yao, K. Yang and Z. Zeng, Electron-transporting boron-doped polycyclic aromatic hydrocarbons: facile synthesis and heteroatom doping positions-modulated optoelectronic properties, *Chin. Chem. Lett.*, 2024, **35**(4), 109117.

10 Y. L. Lai, J. Su, L. X. Wu, D. Luo, X. Z. Wang, X. C. Zhou, C. W. Zhou, X. P. Zhou and D. Li, Selective separation of pyrene from mixed polycyclic aromatic hydrocarbons by a hexahedral metal-organic cage, *Chin. Chem. Lett.*, 2024, **35**(1), 108326.

11 R. Li, G. Xing, H. Li, S. Li and L. Chen, A three-dimensional polycyclic aromatic hydrocarbon based covalent organic framework doped with iodine for electrical conduction, *Chin. Chem. Lett.*, 2023, **34**(4), 107454.

12 W. Qu, W. Yuan, M. Li and Y. Chen, A hexaazatriphenylene fused large discotic polycyclic aromatic hydrocarbon with selective and sensitive metal-ion sensing properties, *Chin. Chem. Lett.*, 2021, **32**(12), 3837–3840.

13 J. Wang, G. Wei, J. Xing and S. Chen, Highly permeable carbon nanotube membranes for efficient surface water treatment through separation and adsorption–electrochemical regeneration, *Journal of Water Process Engineering*, 2024, **64**, 105685.

14 S. Rezania, N. Darajeh, P. F. Rupani, A. Mojiri, H. Kamyab and M. Taghavijeloudar, Recent advances in the adsorption of different pollutants from wastewater using carbon-based and metal-oxide nanoparticles, *Appl. Sci.*, 2024, **14**(24), 11492.

15 A. Chen, S. Xing, Y. Zhang, X. Wei, T. Shen and J. Wang, Simultaneous dual-activation nitrogen-enriched carbon aerogel for efficient adsorption of tetracycline from water, *J. Ind. Eng. Chem.*, 2024, **138**, 175–186.

16 I. Ahmed and S. H. Jhung, Nanoarchitectonics of porous carbon derived from urea-impregnated microporous triazine polymer in KOH activator for adsorptive removal of sulfonamides from water, *J. Ind. Eng. Chem.*, 2025, **143**, 392–402.

17 Y. S. Lee, J. Eom, I. A. Khan and J. O. Kim, The long-term removal of dissolved Mn from drinking water via membrane filtration using sodium permanganate as a pre-oxidant, *J. Ind. Eng. Chem.*, 2024, **130**, 425–435.

18 F. Delkhosh, A. Qotbi, A. H. Behroozi and V. Vatanpour, Magnetron sputtering in membrane fabrication and modification: applications in gas and water treatment, *J. Ind. Eng. Chem.*, 2025, **143**, 85–108.

19 Y. J. Choe, J. Kim, I. S. Choi and S. H. Kim, Metal oxides for Fenton reactions toward radical-assisted water treatment: a review, *J. Ind. Eng. Chem.*, 2025, **142**, 127–140.

20 M. Kazemi, H. Noorizadeh, Y. Jadeja, S. K. Saraswat, R. MM, A. Shankhyan and K. K. Joshi, Advancing CdSe quantum dots for batteries and supercapacitors: electrochemical frontiers, *RSC Adv.*, 2025, **15**(20), 16134–16163.

21 R. S. Dhamorikar, V. G. Lade, P. V. Kewalramani and A. B. Bindwal, Review on integrated advanced oxidation processes for water and wastewater treatment, *J. Ind. Eng. Chem.*, 2024, **138**, 104–122.

22 R. Kumar, A. Sudhaik, D. Kumar, R. Devi, E. Devi, A. Chawla, P. Raizada, C. M. Hussain, T. Ahamad and P. Singh, Synergistic photocatalytic activity of Bi_2O_3/g-C_3N_4/ZnO ternary heterojunction with dual Z-scheme charge transfer towards textile dye degradation, *J. Ind. Eng. Chem.*, 2025, **144**, 575–584.

23 A. Chawla, A. Sudhaik, R. Kumar, P. Raizada, T. Ahamad, A. A. Khan, Q. Van Le, V. H. Nguyen, S. Thakur and P. Singh, Bi_2S_3-based photocatalysts: properties, synthesis, modification strategies, and mechanistic insights towards environmental sustainability and green energy technologies, *Coord. Chem. Rev.*, 2025, **529**, 216443.

24 Q. Wang, X. Yang, Z. Jing, H. Liu, P. Tang, H. Zhu and B. Li, Recent advances in one-dimensional alkali-metal hexatitanate photocatalysts for environmental remediation and solar fuel production, *J. Mater. Sci. Technol.*, 2024, **202**, 201–239.

25 S. Vongehr, S. Tang and X. Meng, Adapting nanotech research as nano-micro hybrids approach biological complexity, a review, *J. Mater. Sci. Technol.*, 2016, **32**(5), 387–401.

26 M. S. Freire, H. J. Silva, G. M. Albuquerque, J. P. Monte, M. T. Lima, J. J. Silva, G. A. Pereira and G. Pereira, Advances on chalcogenide quantum dots-based sensors for environmental pollutants monitoring, *Sci. Total Environ.*, 2024, 172848.

27 W. Yu, H. Chamkouri and L. Chen, Recent advancement on quantum dot-coupled heterojunction structures in catalysis: a review, *Chemosphere*, 2024, 141944.

28 H. E. Ahmed and M. Soylak, Exploring the potential of carbon quantum dots (CQDs) as an advanced nanomaterial for effective sensing and extraction of toxic pollutants, *TrAC, Trends Anal. Chem.*, 2024, 117939.

29 A. T. Ahmed, F. M. Altalbawy, H. R. Al-Hetty, N. Fayzullaev, K. V. Jamuna, J. Sharma, B. Abd, A. M. Ahmed and H. Noorizadeh, Cadmium selenide quantum dots in photo-and electrocatalysis: advances in hydrogen, oxygen, and CO_2 reactions, *Mater. Sci. Semicond. Process.*, 2025, **199**, 109831.

30 B. Zhao, X. Zhang, X. Bai, H. Yang, S. Li, J. Hao, H. Liu, R. Lu, B. Xu, L. Wang and K. Wang, Surface modification toward luminescent and stable silica-coated quantum dots color filter, *Sci. China Mater.*, 2019, **62**(10), 1463–1469.

31 J. Zhang, Y. Zhao, K. Qi and S. Y. Liu, $CuInS_2$ quantum-dot-modified g-C_3N_4 S-scheme heterojunction photocatalyst for hydrogen production and tetracycline degradation, *J. Mater. Sci. Technol.*, 2024, **172**, 145–155.

32 Y. Kim, M. J. Choi and J. Choi, Infrared-harvesting colloidal quantum dot inks for efficient photovoltaics: impact of surface chemistry and device engineering, *J. Mater. Sci. Technol.*, 2023, **147**, 224–240.

33 L. Wang, D. Xu, J. Gao, X. Chen, Y. Duo and H. Zhang, Semiconducting quantum dots: modification and

© 2025 The Author(s). Published by the Royal Society of Chemistry

Environ. Sci.: Adv., 2025, **4**, 1553–1586 | **1579**

applications in biomedical science, *Sci. China Mater.*, 2020, **63**(9), 1631–1650.

34 J. Luo, X. Liu, J. Gu, W. Zhao, M. Gu and Y. Xie, Construction of novel g-C₃N₄/β-FeOOH Z-scheme heterostructure photocatalyst modified with carbon quantum dots for efficient degradation of RhB, *J. Mater. Sci. Technol.*, 2024, **181**, 11–19.

35 F. F. Sead, Y. Jadeja, A. Kumar, M. M. Rekha, M. Kundlas, S. Saini, K. K. Joshi and H. Noorizadeh, Carbon quantum dots for sustainable energy: enhancing electrocatalytic reactions through structural innovation, *Nanoscale Adv.*, 2025, **7**, 3961–3998.

36 Z. Gong, W. Li, S. Zhang, J. Li, H. Su, W. Huang, K. Wang, J. Zhu, X. Zhou, Y. Zhang and T. Guo, Non-contact and non-destructive in-situ inspection for CdSe quantum dot film based on the principle of field-induced photoluminescence quenching, *Sci. China Mater.*, 2024, **67**(11), 3570–3578.

37 N. Syed, J. Huang and Y. Feng, CQDs as emerging trends for future prospect in enhancement of photocatalytic activity, *Carbon Lett.*, 2022, **32**(1), 81–97.

38 M. Kazemi, H. Noorizadeh, Y. Jadeja, S. K. Saraswat, M. M. Rekha, A. Shankhyan and K. K. Joshi, Advancing CdSe quantum dots for batteries and supercapacitors: electrochemical frontiers, *RSC Adv.*, 2025, **15**(20), 16134–16163.

39 J. Chen, D. Liu, M. J. Al-Marri, L. Nuuttila, H. Lehtivuori and K. Zheng, Photo-stability of CsPbBr₃ perovskite quantum dots for optoelectronic application, *Sci. China Mater.*, 2016, **59**(9), 719–727.

40 X. Dong, X. Li, S. Yin, Z. Li, L. Li and J. Li, Regulation of photophysical and electronic properties of I–III–VI quantum dots for light-emitting diodes, *Sci. China Mater.*, 2024, **67**(9), 2737–2748.

41 N. Kundu, D. Sadhukhan and S. Sarkar, Fluorescent carbon nano-materials from coal-based precursors: unveiling structure–function relationship between coal and nano-materials, *Carbon Lett.*, 2022, **32**(3), 671–702.

42 Y. Kumar, T. Chhalodia, P. K. Bedi and P. L. Meena, Photoanode modified with nanostructures for efficiency enhancement in DSSC: a review, *Carbon Lett.*, 2023, **33**(1), 35–58.

43 V. Singh, G. Singla, V. Kansay, V. D. Sharma, A. Bhatia, N. Kumar and M. K. Bera, Luminescent bioplastic nanocomposite based on N, K, Ca-doped carbon quantum dots derived from ice plant flower extract for applications in quantum dot-based optical displays, *Carbon Lett.*, 2025, **35**(3), 1167–1185.

44 Y. J. Oh, M. C. Shin, J. H. Kim and S. J. Yang, Facile preparation of ZnO quantum dots@porous carbon composites through direct carbonization of metal–organic complex for high-performance lithium ion batteries, *Carbon Lett.*, 2021, **31**(2), 323–329.

45 Q. Y. Sun, J. X. Cheng, S. Y. Qi, J. F. Chen and D. Y. Hu, Advances in carbon quantum dot technology for food safety: preparation, modification, applications and mechanisms, *Nano Express*, 2024, **5**(1), 012001.

46 L. Wang, G. Dai, L. Deng and H. Zhong, Progress in semiconductor quantum dots-based continuous-wave laser, *Sci. China Mater.*, 2020, **63**(8), 1382–1397.

47 Y. Liu, Y. Zhou, M. Abdellah, W. Lin, J. Meng, Q. Zhao, S. Yu, Z. Xie, Q. Pan, F. Zhang and T. Pullerits, Inorganic ligands-mediated hole attraction and surface structural reorganization in InP/ZnS QD photocatalysts studied via ultrafast visible and midinfrared spectroscopies, *Sci. China Mater.*, 2022, **65**(9), 2529–2539.

48 M. H. Abdellattif, H. Noorizadeh, S. Al-Hasnaawei, S. Ganesan, A. F. Al-Hussainy, A. Sandhu, A. Sinha and M. Kazemi, Tailoring charge storage mechanisms through TiO₂ quantum dots: a multifunctional strategy for high-performance battery electrodes, *Surf. Interfaces*, 2025, 107164.

49 J. Jiang, N. Li, J. Zou, X. Zhou, G. Eda, Q. Zhang, H. Zhang, L. J. Li, T. Zhai and A. T. Wee, Synergistic additive-mediated CVD growth and chemical modification of 2D materials, *Chem. Soc. Rev.*, 2019, **48**(17), 4639–4654.

50 N. Li, Y. Yang, Z. Shi, Z. Lan, A. Arramel, P. Zhang, W. J. Ong, J. Jiang and J. Lu, Shedding light on the energy applications of emerging 2D hybrid organic-inorganic halide perovskites, *iScience*, 2022, **25**(2), 103862.

51 J. Jiang, F. Li, J. Zou, S. Liu, J. Wang, Y. Zou, K. Xiang, H. Zhang, G. Zhu, Y. Zhang and X. Fu, Three-dimensional MXenes heterostructures and their applications, *Sci. China Mater.*, 2022, **65**(11), 2895–2910.

52 F. Li, J. Jiang, J. Wang, J. Zou, W. Sun, H. Wang, K. Xiang and W. P. Hsu, Porous 3D carbon-based materials: an emerging platform for efficient hydrogen production, *Nano Res.*, 2023, **16**(1), 127–145.

53 N. Song, J. Jiang, S. Hong, Y. Wang, Y. Li and C. Dong, State-of-the-art advancements in single atom electrocatalysts originating from MOFs for electrochemical energy conversion, *Chin. J. Catal.*, 2024, **59**, 38–81.

54 F. Li, G. Zhu, J. Jiang, Y. Yang, L. Deng and X. Li, A review of updated S-scheme heterojunction photocatalysts, *J. Mater. Sci. Technol.*, 2024, **177**, 142–180.

55 J. Jiang, F. Li, L. Ding, C. Zhang, S. Arramel and X. Li, MXenes/CNTs-based hybrids: fabrications, mechanisms, and modification strategies for energy and environmental applications, *Nano Res.*, 2024, **17**(5), 3429–3454.

56 H. Zhou, W. Ye, J. Jiang and Z. Wang, Recent advances on surface modification of non-oxide photocatalysts towards efficient CO₂ conversion, *Carbon Lett.*, 2024, **34**(6), 1569–1591.

57 M. Jouyandeh, S. S. Khadem, S. Habibzadeh, A. Esmaeili, O. Abida, V. Vatanpour, N. Rabiee, M. Bagherzadeh, S. Iravani, M. R. Saeb and R. S. Varma, Quantum dots for photocatalysis: synthesis and environmental applications, *Green Chem.*, 2021, **23**(14), 4931–4954.

58 V. Manikandan and N. Y. Lee, Green synthesis of carbon quantum dots and their environmental applications, *Environ. Res.*, 2022, **212**, 113283.

59 F. F. Sead, J. Makasana, S. K. Saraswat, M. M. Rekha, M. Kundlas, S. Saini, K. K. Joshi and H. Noorizadeh, Electrochemical behavior of carbon quantum dots as

electrolyte additives for enhanced battery and supercapacitor performance, *Mater. Technol.*, 2025, **40**(1), 2500524.

60 L. Cui, C. C. Li, B. Tang and C. Y. Zhang, Advances in the integration of quantum dots with various nanomaterials for biomedical and environmental applications, *Analyst*, 2018, **143**(11), 2469–2478.

61 Q. Xu, W. Cai, W. Li, T. S. Sreeprasad, Z. He, W. J. Ong and N. Li, Two-dimensional quantum dots: fundamentals, photoluminescence mechanism and their energy and environmental applications, *Mater. Today Energy*, 2018, **10**, 222–240.

62 V. G. Reshma and P. V. Mohanan, Quantum dots: applications and safety consequences, *J. Lumin.*, 2019, **205**, 287–298.

63 P. Gupta, G. Tamrakar, S. Biswas, R. S. Dhundhe, V. K. Soni, H. S. Das, P. Sahu, A. K. Chaturwedi, K. Kashyap, T. Akitsu and M. Hait, Quantum dots as a fluorescent sensor for detecting heavy metal ions in aqueous environment: an overview, *ES Chemistry and Sustainability*, 2024, **1**, 1359.

64 F. Farahmandzadeh, K. Kermanshahian, E. Molahosseini and M. Molaei, Efficient mercury ion detection in water: CdTe/CdS/ZnS quantum dots as a simple, sensitive, and rapid fluorescence sensor, *J. Fluoresc.*, 2025, **35**(6), 4829–4840.

65 Y. Zhang, C. Qin, H. Wang, H. Hu and X. Gao, Occurrence, behavior, and ecotoxicity of quantum dots in aquatic environments, *Environ. Sci.: Nano*, 2024, **11**(10), 4044–4059.

66 G. Almeida, R. F. Ubbink, M. Stam, I. du Fossé and A. J. Houtepen, InP colloidal quantum dots for visible and near-infrared photonics, *Nat. Rev. Mater.*, 2023, **8**(11), 742–758.

67 D. Liu, S. Huang, Y. Lu, J. Kang, Z. Zhang, G. Li, S. Wei, L. Wang and B. Zou, Surface metal salt modulating and inner-shell doping of green indium phosphide quantum dots toward high efficiency and narrow emission, *J. Phys. Chem. C*, 2025, **129**(14), 6890–6900.

68 N. Gwak, S. Shin, H. Yoo, G. W. Seo, S. Kim, H. Jang, M. Lee, T. H. Park, B. J. Kim, J. Lim and S. Y. Kim, Highly luminescent shell-less indium phosphide quantum dots enabled by atomistically tailored surface states, *Adv. Mater.*, 2024, **36**(36), 2404480.

69 R. Toufanian, A. Piryatinski, A. H. Mahler, R. Iyer, J. A. Hollingsworth and A. M. Dennis, Bandgap engineering of indium phosphide-based core/shell heterostructures through shell composition and thickness, *Front. Chem.*, 2018, **6**, 567.

70 X. Chen, Y. Guo, J. Li, H. Yang, Z. Chen, D. Luo and X. Liu, Elemental doping tailoring photocatalytic hydrogen evolution of InP/ZnSeS/ZnS quantum dots, *Chem. Eng. J.*, 2024, **496**, 153947.

71 H. S. Chen, C. Y. Chen and Y. C. Wu, High-performance giant InP quantum dots with stress-released morphological ZnSe-ZnSeS-ZnS shell, *Adv. Mater.*, 2025, **37**(3), 2407026.

72 S. M. Click and S. J. Rosenthal, Synthesis, surface chemistry, and fluorescent properties of InP quantum dots, *Chem. Mater.*, 2023, **35**(3), 822–836.

73 S. Wang, J. Li, O. Lin, W. Niu, C. Yang and A. Tang, Development and challenges of indium phosphide-based quantum-dot light-emitting diodes, *J. Photochem. Photobiol., C*, 2023, **55**, 100588.

74 P. Rana, V. Soni, S. Sharma, K. Poonia, S. Patial, P. Singh, V. Selvasembian, V. Chaudhary, C. M. Hussain and P. Raizada, Harnessing nitrogen doped magnetic biochar for efficient antibiotic adsorption and degradation, *J. Ind. Eng. Chem.*, 2025, **148**, 174–195.

75 B. Kaur, P. Singh, A. Singh, Q. Van Le, V. Chaudhary, V. H. Nguyen, M. Asad, A. A. Khan, H. M. Marwani and P. Raizada, Catalytic performance of graphdiyne for CO_2 reduction and charge dynamics progress, *J. Environ. Chem. Eng.*, 2025, 116904.

76 R. Yadav, Y. Kwon, C. Rivaux, C. Saint-Pierre, W. L. Ling and P. Reiss, Narrow near-infrared emission from InP QDs synthesized with indium(I) halides and aminophosphine, *J. Am. Chem. Soc.*, 2023, **145**(10), 5970–5981.

77 B. Chen, D. Li and F. Wang, InP quantum dots: synthesis and lighting applications, *Small*, 2020, **16**(32), 2002454.

78 O. I. Micic, J. R. Sprague, C. J. Curtis, K. M. Jones, J. L. Machol, A. J. Nozik, H. Giessen, B. Fluegel, G. Mohs and N. Peyghambarian, Synthesis and characterization of InP, GaP, and GaInP$_2$ quantum dots, *J. Phys. Chem.*, 1995, **99**(19), 7754–7759.

79 Z. Wu, P. Liu, W. Zhang, K. Wang and X. W. Sun, Development of InP quantum dot-based light-emitting diodes, *ACS Energy Lett.*, 2020, **5**(4), 1095–1106.

80 D. Rajan, B. Manoj, S. Krishna, A. Thomas and K. G. Thomas, The rise of InP quantum dots in nanoscience, *ACS Energy Lett.*, 2025, **10**, 3700–3728.

81 H. Zhang, N. Hu, Z. Zeng, Q. Lin, F. Zhang, A. Tang, Y. Jia, L. S. Li, H. Shen, F. Teng and Z. Du, High-efficiency green InP quantum dot-based electroluminescent device comprising thick-shell quantum dots, *Adv. Opt. Mater.*, 2019, **7**(7), 1801602.

82 P. Liu, Y. Lou, S. Ding, W. Zhang, Z. Wu, H. Yang, B. Xu, K. Wang and X. W. Sun, Green InP/ZnSeS/ZnS core multi-shelled quantum dots synthesized with aminophosphine for effective display applications, *Adv. Funct. Mater.*, 2021, **31**(11), 2008453.

83 H. Van Avermaet, P. Schiettecatte, S. Hinz, L. Giordano, F. Ferrari, C. Nayral, F. Delpech, J. Maultzsch, H. Lange and Z. Hens, Full-spectrum InP-based quantum dots with near-unity photoluminescence quantum efficiency, *ACS Nano*, 2022, **16**(6), 9701–9712.

84 M. D. Tessier, D. Dupont, K. De Nolf, J. De Roo and Z. Hens, Economic and size-tunable synthesis of InP/ZnE (E = S, Se) colloidal quantum dots, *Chem. Mater.*, 2015, **27**(13), 4893–4898.

85 S. Yang, P. Zhao, X. Zhao, L. Qu and X. Lai, InP and Sn:InP based quantum dot sensitized solar cells, *J. Mater. Chem. A*, 2015, **3**(43), 21922–21929.

© 2025 The Author(s). Published by the Royal Society of Chemistry

Environ. Sci.: Adv., 2025, **4**, 1553–1586 | 1581

86 Y. Li, X. Hou, X. Dai, Z. Yao, L. Lv, Y. Jin and X. Peng, Stoichiometry-controlled InP-based quantum dots: synthesis, photoluminescence, and electroluminescence, *J. Am. Chem. Soc.*, 2019, **141**(16), 6448–6452.

87 P. Ramasamy, N. Kim, Y. S. Kang, O. Ramirez and J. S. Lee, Tunable, bright, and narrow-band luminescence from colloidal indium phosphide quantum dots, *Chem. Mater.*, 2017, **29**(16), 6893–6899.

88 S. Tamang, C. Lincheneau, Y. Hermans, S. Jeong and P. Reiss, Chemistry of InP nanocrystal syntheses, *Chem. Mater.*, 2016, **28**(8), 2491–2506.

89 P. Yu, S. Cao, Y. Shan, Y. Bi, Y. Hu, R. Zeng, B. Zou, Y. Wang and J. Zhao, Highly efficient green InP-based quantum dot light-emitting diodes regulated by inner alloyed shell component, *Light: Sci. Appl.*, 2022, **11**(1), 162.

90 P. Ramasamy, B. Kim, M. S. Lee and J. S. Lee, Beneficial effects of water in the colloidal synthesis of InP/ZnS core–shell quantum dots for optoelectronic applications, *Nanoscale*, 2016, **8**(39), 17159–17168.

91 E. Jang, Y. Kim, Y. H. Won, H. Jang and S. M. Choi, Environmentally friendly InP-based quantum dots for efficient wide color gamut displays, *ACS Energy Lett.*, 2020, **5**(4), 1316–1327.

92 R. P. Brown, M. J. Gallagher, D. H. Fairbrother and Z. Rosenzweig, Synthesis and degradation of cadmium-free InP and InPZn/ZnS quantum dots in solution, *Langmuir*, 2018, **34**(46), 13924–13934.

93 W. Zhang, S. Ding, W. Zhuang, W. Wu, P. Liu, X. Qu, H. Liu, H. Yang, Z. Wu, K. Wang and X. W. Sun, InP/ZnS/ZnS core/shell blue quantum dots for efficient light-emitting diodes, *Adv. Funct. Mater.*, 2020, **30**(49), 2005303.

94 J. P. Park, J. J. Lee and S. W. Kim, Highly luminescent InP/GaP/ZnS QDs emitting in the entire color range via a heating up process, *Sci. Rep.*, 2016, **6**, 30094.

95 W. S. Song, H. S. Lee, J. C. Lee, D. S. Jang, Y. Choi, M. Choi and H. Yang, Amine-derived synthetic approach to color-tunable InP/ZnS quantum dots with high fluorescent qualities, *J. Nanopart. Res.*, 2013, **15**, 1750.

96 D. W. Lucey, D. J. MacRae, M. Furis, Y. Sahoo, A. N. Cartwright and P. N. Prasad, Monodispersed InP quantum dots prepared by colloidal chemistry in a noncoordinating solvent, *Chem. Mater.*, 2005, **17**(14), 3754–3762.

97 M. J. Seong, O. I. Mićić, A. J. Nozik, A. Mascarenhas and H. M. Cheong, Size-dependent Raman study of InP quantum dots, *Appl. Phys. Lett.*, 2003, **82**(2), 185–187.

98 J. H. Jo, J. H. Kim, K. H. Lee, C. Y. Han, E. P. Jang, Y. R. Do and H. Yang, High-efficiency red electroluminescent device based on multishelled InP quantum dots, *Opt. Lett.*, 2016, **41**(17), 3984–3987.

99 J. Park, S. Kim, S. Kim, Y. S. Yu, S. T. Lee, B. Kim and S. W. Kim, Fabrication of highly luminescent InP/Cd and InP/CdS quantum dots, *J. Lumin.*, 2010, **130**(10), 1825–1828.

100 Y. Hai, K. Gahlot, M. Tanchev, S. Mutalik, E. K. Tekelenburg, J. Hong, M. Ahmadi, L. Piveteau, M. A. Loi and L. Protesescu, Metal–solvent complex

formation at the surface of InP colloidal quantum dots, *J. Am. Chem. Soc.*, 2024, **146**(18), 12808–12818.

101 K. T. Yong, H. Ding, I. Roy, W. C. Law, E. J. Bergey, A. Maitra and P. N. Prasad, Imaging pancreatic cancer using bioconjugated InP quantum dots, *ACS Nano*, 2009, **3**(3), 502–510.

102 L. Yan, Z. Chen, Y. Bai, W. Liu, H. He and C. He, First-principles study on strain-induced modulation of electronic properties in indium phosphide, *Nanomaterials*, 2024, **14**(21), 1756.

103 M. Stam, G. Almeida, R. F. Ubbink, L. M. van der Poll, Y. B. Vogel, H. Chen, L. Giordano, P. Schiettecatte, Z. Hens and A. J. Houtepen, Near-unity photoluminescence quantum yield of core-only InP quantum dots via a simple postsynthetic InF_3 treatment, *ACS Nano*, 2024, **18**(22), 14685–14695.

104 J. Lim, M. Park, W. K. Bae, D. Lee, S. Lee, C. Lee and K. Char, Highly efficient cadmium-free quantum dot light-emitting diodes enabled by the direct formation of excitons within InP@ZnSeS quantum dots, *ACS Nano*, 2013, **7**(10), 9019–9026.

105 C. Zhang, Y. Liu, Y. Zhao, Y. Qu, L. Wang, H. Zhang, D. Chen and J. Wang, Synthesis of InP quantum dots loaded on $Ti_3C_2T_x$ MXene for high-efficiency photocatalytic hydrogen peroxide production in water, *J. Alloys Compd.*, 2025, 180937.

106 H. Chibli, L. Carlini, S. Park, N. M. Dimitrijevic and J. L. Nadeau, Cytotoxicity of InP/ZnS quantum dots related to reactive oxygen species generation, *Nanoscale*, 2011, **3**(6), 2552–2559.

107 T. A. Gazis, A. J. Cartlidge and P. D. Matthews, Colloidal III–V quantum dots: a synthetic perspective, *J. Mater. Chem. C*, 2023, **11**(12), 3926–3935.

108 D. C. Gary, M. W. Terban, S. J. Billinge and B. M. Cossairt, Two-step nucleation and growth of InP quantum dots via magic-sized cluster intermediates, *Chem. Mater.*, 2015, **27**(4), 1432–1441.

109 D. H. Kwak, P. Ramasamy, Y. S. Lee, M. H. Jeong and J. S. Lee, High-performance hybrid InP QDs/black phosphorus photodetector, *ACS Appl. Mater. Interfaces*, 2019, **11**(32), 29041–29046.

110 D. Liu, S. Huang, Y. Lu, J. Kang, Z. Zhang, G. Li, S. Wei, L. Wang and B. Zou, Surface metal salt modulating and inner-shell doping of green indium phosphide quantum dots toward high efficiency and narrow emission, *J. Phys. Chem. C*, 2025, **129**(14), 6890–6900.

111 X. Duan, J. Ma, W. Zhang, P. Liu, H. Liu, J. Hao, K. Wang, L. Samuelson and X. W. Sun, Study of the interfacial oxidation of InP quantum dots synthesized from tris(dimethylamino)phosphine, *ACS Appl. Mater. Interfaces*, 2022, **15**(1), 1619–1628.

112 F. Cao, S. Wang, F. Wang, Q. Wu, D. Zhao and X. Yang, A layer-by-layer growth strategy for large-size InP/ZnSe/ZnS core–shell quantum dots enabling high-efficiency light-emitting diodes, *Chem. Mater.*, 2018, **30**(21), 8002–8007.

113 C. Ippen, T. Greco and A. Wedel, InP/ZnSe/ZnS: a novel multishell system for InP quantum dots for improved

luminescence efficiency and its application in a light-emitting device, *J. Inf. Disp.*, 2012, **13**(2), 91–95.

114 P. Chen, H. Liu, Y. Cui, C. Liu, Y. Li, Y. Gao, J. Cheng and T. He, Inner shell influence on the optical properties of InP/ZnSeS/ZnS quantum dots, *J. Phys. Chem. C*, 2023, **127**(5), 2464–2470.

115 J. Liu, S. Yue, H. Zhang, C. Wang, D. Barba, F. Vidal, S. Sun, Z. M. Wang, J. Bao, H. Zhao and G. S. Selopal, Efficient photoelectrochemical hydrogen generation using eco-friendly "giant" InP/ZnSe core/shell quantum dots, *ACS Appl. Mater. Interfaces*, 2023, **15**(29), 34797–34808.

116 J. H. Jo, D. Y. Jo, S. H. Lee, S. Y. Yoon, H. B. Lim, B. J. Lee, Y. R. Do and H. Yang, InP-based quantum dots having an InP core, composition-gradient ZnSeS inner shell, and ZnS outer shell with sharp, bright emissivity, and blue absorptivity for display devices, *ACS Appl. Nano Mater.*, 2020, **3**(2), 1972–1980.

117 Y. H. Suh, S. Lee, J. Jung, S. M. Bang, S. Y. Yang, J. Fan, X. B. Zhan, S. Samarakoon, C. Jo, J. W. Kim, Y. Choi and H. W. Choi, Engineering core size of InP quantum dot with incipient ZnS for blue emission, *Adv. Opt. Mater.*, 2022, **10**(7), 2102372.

118 J. H. Jo, J. H. Kim, S. H. Lee, H. S. Jang, D. S. Jang, J. C. Lee, K. U. Park, Y. Choi, C. Ha and H. Yang, Photostability enhancement of InP/ZnS quantum dots enabled by In$_2$O$_3$ overcoating, *J. Alloys Compd.*, 2015, **647**, 6–13.

119 C. C. Huang, S. R. Chung and K. W. Wang, Enhancing optical properties through zinc halide precursor selection: interfacial optimization of InZnP quantum dots, *J. Mater. Chem. C*, 2024, **12**(4), 1317–1324.

120 W. M. Schulz, R. Robach, M. Reischle, G. J. Beirne, M. Bommer, M. Jetter and P. Michler, Optical and structural properties of InP quantum dots embedded in (Al$_x$Ga$_{1-x}$)$_{0.51}$In$_{0.49}$P, *Phys. Rev. B: Condens. Matter Mater. Phys.*, 2009, **79**(3), 035329.

121 P. M. Allen, B. J. Walker and M. G. Bawendi, Mechanistic insights into the formation of InP quantum dots, *Angew. Chem., Int. Ed.*, 2010, **49**(4), 760–762.

122 J. Wang, B. Ba, J. Meng, S. Yang, S. Tian, M. Zhang, F. Huang, K. Zheng, T. Pullerits and J. Tian, Transition layer assisted synthesis of defect-free amine-phosphine based InP QDs, *Nano Lett.*, 2024, **24**(29), 8894–8901.

123 S. Lee, L. K. Sagar, X. Li, Y. Dong, B. Chen, Y. Gao, D. Ma, L. Levina, A. Grenville, S. Hoogland and F. P. García de Arquer, InP-quantum-dot-in-ZnS-matrix solids for thermal and air stability, *Chem. Mater.*, 2020, **32**(22), 9584–9590.

124 K. C. Dümbgen, J. Zito, I. Infante and Z. Hens, Shape, electronic structure, and trap states in indium phosphide quantum dots, *Chem. Mater.*, 2021, **33**(17), 6885–6896.

125 M. D. Tessier, K. De Nolf, D. Dupont, D. Sinnaeve, J. De Roo and Z. Hens, Aminophosphines: a double role in the synthesis of colloidal indium phosphide quantum dots, *J. Am. Chem. Soc.*, 2016, **138**(18), 5923–5929.

126 P. Ramasamy, K. J. Ko, J. W. Kang and J. S. Lee, Two-step "seed-mediated" synthetic approach to colloidal indium phosphide quantum dots with high-purity photo- and

electroluminescence, *Chem. Mater.*, 2018, **30**(11), 3643–3647.

127 F. Lelarge, B. Dagens, J. Renaudier, R. Brenot, A. Accard, F. van Dijk, D. Make, O. Le Gouezigou, J. G. Provost, F. Poingt and J. Landreau, Recent advances on InAs/InP quantum dash based semiconductor lasers and optical amplifiers operating at 1.55 μm, *IEEE J. Sel. Top. Quantum Electron.*, 2007, **13**(1), 111–124.

128 M. Levy, J. R. Bertram, K. A. Eller, A. Chatterjee and P. Nagpal, Near-infrared-light-triggered antimicrobial indium phosphide quantum dots, *Angew. Chem., Int. Ed.*, 2019, **131**(33), 11536–11540.

129 S. S. Chopra and T. L. Theis, Comparative cradle-to-gate energy assessment of indium phosphide and cadmium selenide quantum dot displays, *Environ. Sci.: Nano*, 2017, **4**(1), 244–254.

130 A. Thomas, P. V. Nair and K. G. Thomas, InP quantum dots: an environmentally friendly material with resonance energy transfer requisites, *J. Phys. Chem. C*, 2014, **118**(7), 3838–3845.

131 M. Abbasi, R. Aziz, M. T. Rafiq, A. U. Bacha, Z. Ullah, A. Ghaffar, G. Mustafa, I. Nabi and M. T. Hayat, Efficient performance of InP and InP/ZnS quantum dots for photocatalytic degradation of toxic aquatic pollutants, *Environ. Sci. Pollut. Res.*, 2024, **31**(13), 19986–20000.

132 Y. H. Won, O. Cho, T. Kim, D. Y. Chung, T. Kim, H. Chung, H. Jang, J. Lee, D. Kim and E. Jang, Highly efficient and stable InP/ZnSe/ZnS quantum dot light-emitting diodes, *Nature*, 2019, **575**(7784), 634–638.

133 Y. Xu, Y. Lv, R. Wu, H. Shen, H. Yang, H. Zhang, J. Li and L. S. Li, Preparation of highly stable and photoluminescent cadmium-free InP/GaP/ZnS core/shell quantum dots and application to quantitative immunoassay, *Part. Part. Syst. Charact.*, 2020, **37**(3), 1900441.

134 S. Wang, J. Li, O. Lin, W. Niu, C. Yang and A. Tang, Development and challenges of indium phosphide-based quantum-dot light-emitting diodes, *J. Photochem. Photobiol., C*, 2023, **55**, 100588.

135 J. L. Stein, W. M. Holden, A. Venkatesh, M. E. Mundy, A. J. Rossini, G. T. Seidler and B. M. Cossairt, Probing surface defects of InP quantum dots using phosphorus Kα and Kβ X-ray emission spectroscopy, *Chem. Mater.*, 2018, **30**(18), 6377–6388.

136 S. Koh, T. Eom, W. D. Kim, K. Lee, D. Lee, Y. K. Lee, H. Kim, W. K. Bae and D. C. Lee, Zinc–phosphorus complex working as an atomic valve for colloidal growth of monodisperse indium phosphide quantum dots, *Chem. Mater.*, 2017, **29**(15), 6346–6355.

137 A. M. Saeboe, J. Kays, A. H. Mahler and A. M. Dennis, Pushing indium phosphide quantum dot emission deeper into the near infrared, in *Colloidal Nanoparticles for Biomedical Applications XIII*, 2018, vol. 10507, pp. 156–164.

138 H. S. Shim, M. Ko, S. Nam, S. Oh, J. H. Jeong, S. Yang, Y. R. Park, S. M. Do and J. K. Song, InP/ZnSeS/ZnS quantum dots with high quantum yield and color purity

© 2025 The Author(s). Published by the Royal Society of Chemistry

Environ. Sci.: Adv., 2025, **4**, 1553–1586 | **1583**

for display devices, *ACS Appl. Nano Mater.*, 2023, **6**(2), 1285–1294.

139 X. Zhou, Q. Hu and Y. Wang, Magnesium ions enhanced core-shell lattice matching for narrow-band green emission indium phosphide QDs, *Chem. Eng. J.*, 2024, **488**, 151152.

140 H. Chen, J. Chen, Y. Wu, W. Xie and L. Jin, A study on the mechanism of indium phosphide/zinc sulfide core/shell quantum dots influencing embryo incubation of rare minnow (Gobiocypris rarus), *Aquat. Toxicol.*, 2023, **261**, 106593.

141 O. B. Achorn, D. Franke and M. G. Bawendi, Seedless continuous injection synthesis of indium phosphide quantum dots as a route to large size and low size dispersity, *Chem. Mater.*, 2020, **32**(15), 6532–6539.

142 S. K. Lee and E. J. McLaurin, Recent advances in colloidal indium phosphide quantum dot production, *Curr. Opin. Green Sustainable Chem.*, 2018, **12**, 76–82.

143 S. Tamang, K. D. Wegner and P. Reiss, Quantum dot material systems, compositional families, in *Quantum Dot Display Science and Technology*, 2025, pp. 23–80.

144 A. Dalui, K. Ariga and S. Acharya, Colloidal semiconductor nanocrystals: from bottom-up nanoarchitectonics to energy harvesting applications, *Chem. Commun.*, 2023, **59**(73), 10835–10865.

145 A. Soosaimanickam, P. Manidurai, S. Krishna Sundaram and M. B. Sridharan, Advancements and challenges in synthesizing colloidal semiconductor nanocrystals by hot-injection method, in *Nanomaterials: The Building Blocks of Modern Technology: Synthesis, Properties and Applications*, 2023, pp. 143–179.

146 S. Sambyal, A. Sudhaik, N. Sonu, P. Raizada, V. Chaudhary, V. H. Nguyen, A. A. Khan, C. M. Hussain and P. Singh, Recent updates on cadmium indium sulfide (CdIn$_2$S$_4$ or CIS) photo-catalyst: synthesis, enhancement strategies and applications, *Coord. Chem. Rev.*, 2025, **535**, 216653.

147 Q. Hou, Y. Huang, J. Kong, Z. Zhang, A. A. Sergeev, Z. Peng, Z. Sun, J. Tang, A. L. Rogach and Z. Du, Shell composition-mediated band alignment and defect engineering in indium phosphide-based core/shell quantum dots, *J. Phys. Chem. C*, 2025, **129**(14), 6890–6900.

148 S. B. Brichkin, Synthesis and properties of colloidal indium phosphide quantum dots, *Colloid J.*, 2015, **77**, 393–403.

149 R. W. Epps, F. Delgado-Licona, H. Yang, T. Kim, A. A. Volk, S. Han, S. Jun and M. Abolhasani, Accelerated multi-stage synthesis of indium phosphide quantum dots in modular flow reactors, *Adv. Mater. Technol.*, 2023, **8**(4), 2201845.

150 C. Ippen, B. Schneider, C. Pries, S. Kröpke, T. Greco and A. Holländer, Large-scale synthesis of high quality InP quantum dots in a continuous flow-reactor under supercritical conditions, *Nanotechnology*, 2015, **26**(8), 085604.

151 S. K. Lee and E. J. McLaurin, Recent advances in colloidal indium phosphide quantum dot production, *Curr. Opin. Green Sustainable Chem.*, 2018, **12**, 76–82.

152 S. B. Brichkin, Synthesis and properties of colloidal indium phosphide quantum dots, *Colloid J.*, 2015, **77**, 393–403.

153 D. Marşan, H. Şengül and A. M. Özdil, Comparative assessment of the phase transfer behaviour of InP/ZnS and CuInS/ZnS quantum dots and CdSe/ZnS quantum dots under varying environmental conditions, *Environ. Sci.: Nano*, 2019, **6**(3), 879–891.

154 T. R. Kuo, S. T. Hung, Y. T. Lin, T. L. Chou, M. C. Kuo, Y. P. Kuo and C. C. Chen, Green synthesis of InP/ZnS core/shell quantum dots for application in heavy-metal-free light-emitting diodes, *Nanoscale Res. Lett.*, 2017, **12**, 1–7.

155 O. B. Achorn, D. Franke and M. G. Bawendi, Seedless continuous injection synthesis of indium phosphide quantum dots as a route to large size and low size dispersity, *Chem. Mater.*, 2020, **32**(15), 6532–6539.

156 J. C. Kays, A. M. Saeboe, R. Toufanian, D. E. Kurant and A. M. Dennis, Shell-free copper indium sulfide quantum dots induce toxicity in vitro and in vivo, *Nano Lett.*, 2020, **20**(3), 1980–1991.

157 L. Li, Y. Chen, G. Xu, D. Liu, Z. Yang, T. Chen, X. Wang, J. Jiang, D. Xue and G. Lin, In vivo comparison of the biodistribution and toxicity of InP/ZnS quantum dots with different surface modifications, *Int. J. Nanomed.*, 2020, 1951–1965.

158 L. Li, T. Chen, Z. Yang, Y. Chen, D. Liu, H. Xiao, M. Liu, K. Liu, J. Xu, S. Liu and X. Wang, Nephrotoxicity evaluation of indium phosphide quantum dots with different surface modifications in BALB/c mice, *Int. J. Mol. Sci.*, 2020, **21**(19), 7137.

159 R. Toufanian, M. Chern, V. H. Kong and A. M. Dennis, Engineering brightness-matched indium phosphide quantum dots, *Chem. Mater.*, 2021, **33**(6), 1964–1975.

160 M. Allocca, L. Mattera, A. Bauduin, B. Miedziak, M. Moros, L. De Trizio, A. Tino, P. Reiss, A. Ambrosone and C. Tortiglione, An integrated multilevel analysis profiling biosafety and toxicity induced by indium- and cadmium-based quantum dots in vivo, *Environ. Sci. Technol.*, 2019, **53**(7), 3938–3947.

161 R. J. Huang, Z. K. Qin, L. L. Shen, G. Lv, F. Tao, J. Wang and Y. J. Gao, Interface engineering of InP/ZnS core/shell quantum dots for exceptional photocatalytic H$_2$ evolution, *J. Mater. Chem. A*, 2023, **11**(12), 6217–6225.

162 K. D. Wegner, F. Dussert, D. Truffier-Boutry, A. Benayad, D. Beal, L. Mattera, W. L. Ling, M. Carrière and P. Reiss, Influence of the core/shell structure of indium phosphide based quantum dots on their photostability and cytotoxicity, *Front. Chem.*, 2019, **7**, 466.

163 D. Liu, S. Huang, Y. Lu, J. Kang, Z. Zhang, G. Li, S. Wei, L. Wang and B. Zou, Surface metal salt modulating and inner-shell doping of green indium phosphide quantum dots toward high efficiency and narrow emission, *J. Phys. Chem. C*, 2025, **129**(14), 6890–6900.

164 C. Zhang, X. Chen, Y. Liu, Y. Zhao, H. Zhang, D. Chen, Z. Zong and J. Wang, Synthesis of InP quantum dot decorated Bi$_2$WO$_6$ microspheres for the efficient photocatalytic production of hydrogen peroxide in water, *J. Alloys Compd.*, 2025, **1011**, 178253.

1584 | *Environ. Sci.: Adv.*, 2025, **4**, 1553–1586

© 2025 The Author(s). Published by the Royal Society of Chemistry

165 X. Duan, J. Ma, W. Zhang, P. Liu, H. Liu, J. Hao, K. Wang, L. Samuelson and X. W. Sun, Study of the interfacial oxidation of InP quantum dots synthesized from tris(dimethylamino)phosphine, *ACS Appl. Mater. Interfaces*, 2022, **15**(1), 1619–1628.

166 S. Zeng, W. Tan, J. Si, L. Mao, J. Shi, Y. Li and X. Hou, Ultrafast electron transfer in InP/ZnSe/ZnS quantum dots for photocatalytic hydrogen evolution, *J. Phys. Chem. Lett.*, 2022, **13**(39), 9096–9102.

167 D. Xu, L. L. Shen, Z. K. Qin, S. Yan, N. Wang, J. Wang and Y. J. Gao, Construction of reverse type-II InP/Zn$_x$Cd$_{1-x}$S core/shell quantum dots with low interface strain to enhance photocatalytic hydrogen evolution, *Inorg. Chem.*, 2024, **63**(27), 12582–12592.

168 S. Yu, X. B. Fan, X. Wang, J. Li, Q. Zhang, A. Xia, S. Wei, L. Z. Wu, Y. Zhou and G. R. Patzke, Efficient photocatalytic hydrogen evolution with ligand engineered all-inorganic InP and InP/ZnS colloidal quantum dots, *Nat. Commun.*, 2018, **9**(1), 4009.

169 X. Chen, Y. Guo, J. Li, H. Yang, Z. Chen, D. Luo and X. Liu, Elemental doping tailoring photocatalytic hydrogen evolution of InP/ZnSeS/ZnS quantum dots, *Chem. Eng. J.*, 2024, **496**, 153947.

170 D. Stone, S. Gigi, T. Naor, X. Li and U. Banin, Size-dependent photocatalysis by wurtzite InP quantum dots utilizing the red spectral region, *ACS Energy Lett.*, 2024, **9**(12), 5907–5913.

171 B. Chon, S. Choi, Y. Seo, H. S. Lee, C. H. Kim, H. J. Son and S. O. Kang, InP-quantum dot surface-modified TiO$_2$ catalysts for sustainable photochemical carbon dioxide reduction, *ACS Sustain. Chem. Eng.*, 2022, **10**(18), 6033–6044.

172 Y. Cao, Q. Zheng, Z. Rao, Z. Zhang, R. Xie, S. Yu and Y. Zhou, InP quantum dots on g-C$_3$N$_4$ nanosheets to promote molecular oxygen activation under visible light, *Chin. Chem. Lett.*, 2020, **31**(10), 2689–2692.

173 H. Kwon, S. Kim, S. B. Kang and J. Bang, Preparation of InP quantum dots-TiO$_2$ nanoparticle composites with enhanced visible light induced photocatalytic activity, *CrystEngComm*, 2022, **24**(20), 3724–3730.

174 A. Rezvani, Z. Wang, K. D. Wegner, H. Soltanmoradi, A. Kichigin, X. Zhou, T. Gantenberg, J. Schram, B. A. Zubiri, E. Spiecker and J. Walter, Separation of indium phosphide/zinc sulfide core–shell quantum dots from shelling byproducts through multistep agglomeration, *ACS Nano*, 2025, **19**(20), 19080–19094.

175 D. Xu, L. L. Shen, Z. K. Qin, S. Yan, N. Wang, J. Wang and Y. J. Gao, Construction of reverse type-II InP/Zn$_x$Cd$_{1-x}$S core/shell quantum dots with low interface strain to enhance photocatalytic hydrogen evolution, *Inorg. Chem.*, 2024, **63**(27), 12582–12592.

176 A. Tran, R. Valleix, M. Matic, M. Sleiman, F. Cisnetti and D. Boyer, Environmentally friendly InP quantum dots as a visible-light catalyst for water treatment, *Environ. Sci.: Nano*, 2023, **10**(7), 1749–1753.

177 P. Huo, X. Shi, W. Zhang, P. Kumar and B. Liu, An overview on the incorporation of graphene quantum dots on TiO$_2$ for

178 L. Gnanasekaran, R. Hemamalini and K. Ravichandran, Synthesis and characterization of TiO$_2$ quantum dots for photocatalytic application, *J. Saudi Chem. Soc.*, 2015, **19**(5), 589–594.

179 V. A. Fonoberov and A. A. Balandin, ZnO quantum dots: physical properties and optoelectronic applications, *J. Nanoelectron. Optoelectron.*, 2006, **1**(1), 19–38.

180 V. N. Kalpana and V. Devi Rajeswari, A review on green synthesis, biomedical applications, and toxicity studies of ZnO NPs, *Bioinorg. Chem. Appl.*, 2018, **2018**, 3569758.

181 J. Wang, J. Jiang, F. Li, J. Zou, K. Xiang, H. Wang, Y. Li and X. Li, Emerging carbon-based quantum dots for sustainable photocatalysis, *Green Chem.*, 2023, **25**(1), 32–58.

182 X. Guan, Z. Li, X. Geng, Z. Lei, A. Karakoti, T. Wu, P. Kumar, J. Yi and A. Vinu, Emerging trends of carbon-based quantum dots: nanoarchitectonics and applications, *Small*, 2023, **19**(17), 2207181.

183 S. S. Chopra and T. L. Theis, Comparative cradle-to-gate energy assessment of indium phosphide and cadmium selenide quantum dot displays, *Environ. Sci.: Nano*, 2017, **4**(1), 244–254.

184 K. J. McHugh, L. Jing, A. M. Behrens, S. Jayawardena, W. Tang, M. Gao, R. Langer and A. Jaklenec, Biocompatible semiconductor quantum dots as cancer imaging agents, *Adv. Mater.*, 2018, **30**(18), 1706356.

185 L. Dirheimer, T. Pons, F. Marchal and L. Bezdetnaya, Quantum dots mediated imaging and phototherapy in cancer spheroid models: state of the art and perspectives, *Pharmaceutics*, 2022, **14**(10), 2136.

186 F. Liu, Y. Ge, Y. Xing, D. Ren and N. Ho, Multicolored carbon quantum dots-based expanded fluorescence strategy for high-throughput detection of various water pollutants, *ACS ES&T Eng.*, 2024, **4**(10), 2415–2423.

187 B. Xu, J. Zhou, Z. Zhang, C. Chang and Y. Deng, Research progress on quantum dot-embedded polymer films and plates for LCD backlight display, *Polymers*, 2025, **17**(2), 233.

188 M. Abbasi, Synthesis and development of metal doped quantum dots for environmental remediation, Doctoral dissertation, Fatima Jinnah Women University, Rawalpindi, 2024.

189 P. R. Chen, M. S. Hoang, K. Y. Lai and H. S. Chen, Bifunctional metal oleate as an alternative method to remove surface oxide and passivate surface defects of aminophosphine-based InP quantum dots, *Nanomaterials*, 2022, **12**(3), 573.

190 A. Saha, R. Yadav, C. Rivaux, D. Aldakov and P. Reiss, Water-soluble alumina-coated indium phosphide core–shell quantum dots with efficient deep-red emission beyond 700 nm, *Small*, 2024, **20**(45), 2404426.

191 J. Zhao, R. Jiang, M. Huang, Y. Qiao, S. Wang, W. Zhang, T. Tian, J. Wang, R. Guo and S. Mei, Advancing ecofriendly indium phosphide quantum dots: comprehensive strategies toward color-pure luminescence

enhanced performances, *J. Mater. Sci.*, 2021, **56**(10), 6031–6051.

© 2025 The Author(s). Published by the Royal Society of Chemistry

Environ. Sci.: Adv., 2025, **4**, 1553–1586 | **1585**

for wide color gamut displays, *ACS Energy Lett.*, 2025, **10**(5), 2096–2132.

192 A. Stelmakh, G. Marnieros, E. Schrader, G. Nedelcu, O. Hordiichuk, E. Rusanov, I. Cherniukh, D. Zindel, H. Grutzmacher and M. V. Kovalenko, Acylphosphine route to colloidal InP quantum dots, *J. Am. Chem. Soc.*, 2025, **147**(13), 11446–11455.

193 L. Xie, D. K. Harris, M. G. Bawendi and K. F. Jensen, Effect of trace water on the growth of indium phosphide quantum dots, *Chem. Mater.*, 2015, **27**(14), 5058–5063.

194 H. A. Nguyen, F. Y. Dou, N. Park, W. Wu, S. Sarsito, H. Diakubama, H. Larson, E. Nishiwaki, M. Homer, M. Cash and B. M. Cossairt, Predicting indium phosphide quantum dot properties from synthetic procedures using machine learning, *Chem. Mater.*, 2022, **34**(14), 6296–6311.

195 A. Tarantini, K. D. Wegner, F. Dussert, G. Sarret, D. Beal, L. Mattera, C. Lincheneau, O. Proux, D. Truffier-Boutry, C. Moriscot and B. Gallet, Physicochemical alterations and toxicity of InP alloyed quantum dots aged in environmental conditions: a safer by design evaluation, *NanoImpact*, 2019, **14**, 100168.

196 E. A. Baquero, H. Virieux, R. A. Swain, A. Gillet, A. Cros-Gagneux, Y. Coppel, B. Chaudret, C. Nayral and F. Delpech, Synthesis of oxide-free InP quantum dots: surface control and H₂-assisted growth, *Chem. Mater.*, 2017, **29**(22), 9623–9627.

197 H. J. Byun, J. C. Lee and H. Yang, Solvothermal synthesis of InP quantum dots and their enhanced luminescent efficiency by post-synthetic treatments, *J. Colloid Interface Sci.*, 2011, **355**(1), 35–41.

198 E. M. Janke, N. E. Williams, C. She, D. Zherebetskyy, M. H. Hudson, L. Wang, D. J. Gosztola, R. D. Schaller, B. Lee, C. Sun and G. S. Engel, Origin of broad emission spectra in InP quantum dots: contributions from structural and electronic disorder, *J. Am. Chem. Soc.*, 2018, **140**(46), 15791–15803.

199 K. Wu, N. Song, Z. Liu, H. Zhu, W. Rodríguez-Córdoba and T. Lian, Interfacial charge separation and recombination in InP and quasi-type II InP/CdS core/shell quantum dot-molecular acceptor complexes, *J. Phys. Chem. A*, 2013, **117**(32), 7561–7570.

200 R. F. Ubbink, G. Almeida, H. Iziyi, I. du Fossé, R. Verkleij, S. Ganapathy, E. R. Van Eck and A. J. Houtepen, A water-free in situ HF treatment for ultrabright InP quantum dots, *Chem. Mater.*, 2022, **34**(22), 10093–10103.

201 I. K. Litvinov, T. N. Belyaeva, A. V. Salova, N. D. Aksenov, E. A. Leontieva, A. O. Orlova and E. S. Kornilova, Quantum dots based on indium phosphide (InP): the effect of chemical modifications of the organic shell on interaction with cultured cells of various origins, *Cell Tissue Biol.*, 2018, **12**(2), 135–145.

202 P. J. Poole, K. Kaminska, P. Barrios, Z. Lu and J. Liu, Growth of InAs/InP-based quantum dots for 1.55 μm laser applications, *J. Cryst. Growth*, 2009, **311**(6), 1482–1486.

203 S. Rakshit, B. Cohen, M. Gutiérrez, A. El-Ballouli and A. Douhal, Deep blue and highly emissive ZnS-passivated InP QDs: facile synthesis, characterization, and deciphering of their ultrafast-to-slow photodynamics, *ACS Appl. Mater. Interfaces*, 2023, **15**(2), 3099–3111.

204 O. I. Mićić, S. P. Ahrenkiel and A. J. Nozik, Synthesis of extremely small InP quantum dots and electronic coupling in their disordered solid films, *Appl. Phys. Lett.*, 2001, **78**(25), 4022–4024.

205 A. H. Proppe, D. B. Berkinsky, H. Zhu, T. Šverko, A. E. Kaplan, J. R. Horowitz, T. Kim, H. Chung, S. Jun and M. G. Bawendi, Highly stable and pure single-photon emission with 250 ps optical coherence times in InP colloidal quantum dots, *Nat. Nanotechnol.*, 2023, **18**(9), 993–999.

206 J. L. Blackburn, D. C. Selmarten, R. J. Ellingson, M. Jones, O. Micic and A. J. Nozik, Electron and hole transfer from indium phosphide quantum dots, *J. Phys. Chem. B*, 2005, **109**(7), 2625–2631.

207 S. Bai, M. Yang, J. Jiang, X. He, J. Zou, Z. Xiong, G. Liao and S. Liu, Recent advances of MXenes as electrocatalysts for hydrogen evolution reaction, *npj 2D Mater. Appl.*, 2021, **5**(1), 78.

208 J. Zou, J. Wu, Y. Wang, F. Deng, J. Jiang, Y. Zhang, S. Liu, N. Li, H. Zhang, J. Yu and T. Zhai, Additive-mediated intercalation and surface modification of MXenes, *Chem. Soc. Rev.*, 2022, **51**(8), 2972–2990.

209 R. W. Crisp, N. Kirkwood, G. Grimaldi, S. Kinge, L. D. Siebbeles and A. J. Houtepen, Highly photoconductive InP quantum dots films and solar cells, *ACS Appl. Energy Mater.*, 2018, **1**(11), 6569–6576.

210 T. Zhao, Q. Zhao, J. Lee, S. Yang, H. Wang, C. M. Chuang, M. Y. He, S. M. Thompson, G. Liu, N. Oh and C. B. Murray, Engineering the surface chemistry of colloidal InP quantum dots for charge transport, *Chem. Mater.*, 2022, **34**(18), 8306–8315.

211 R. Subagyo, A. Yudhowijoyo, N. A. Sholeha, S. S. Hutagalung, D. Prasetyoko, M. D. Birowosuto, L. Arramel, J. Jiang and Y. Kusumawati, Recent advances of modification effect in Co₃O₄-based catalyst towards highly efficient photocatalysis, *J. Colloid Interface Sci.*, 2023, **650**, 1550–1590.

212 F. Li, Y. Anjarsari, J. Wang, R. Azzahiidah, J. Jiang, J. Zou, K. Xiang, H. Ma and B. Arramel, Modulation of the lattice structure of 2D carbon-based materials for improving photo/electric properties, *Carbon Lett.*, 2023, **33**(5), 1321–1331.

213 J. Wang, Q. Qin, F. Li, Y. Anjarsari, W. Sun, R. Azzahiidah, J. Zou, K. Xiang, H. Ma, J. Jiang and S. Arramel, Recent advances of MXenes Mo₂C-based materials for efficient photocatalytic hydrogen evolution reaction, *Carbon Lett.*, 2023, **33**(5), 1381–1394.